



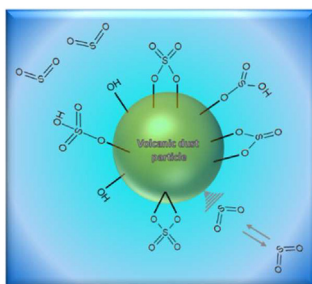
ELSEVIER

Contents lists available at ScienceDirect

Atmospheric Environment

journal homepage: www.elsevier.com/locate/atmosenvUptake and surface chemistry of SO₂ on natural volcanic dustsD. Urupina^{a,*}, J. Lasne^a, M.N. Romanias^a, V. Thiery^b, P. Dagsson-Waldhauserova^{c,d}, F. Thevenet^a^a IMT Lille Douai, Univ. Lille, SAGE, 59000, Lille, France^b IMT Lille Douai, Univ. Lille, GCE, 59000, Lille, France^c Agricultural University of Iceland, Keldnaholt, Reykjavik, 112, Iceland^d Faculty of Environmental Sciences, Czech University of Life Sciences, Prague, 165 21, Czech Republic

GRAPHICAL ABSTRACT



ARTICLE INFO

Keywords:

V-dust
Heterogeneous reactions
Sulfur dioxide
Sulfate formation
Uptake coefficient
DRIFTS

ABSTRACT

V-dust (v-dust) is a highly variable source of natural particles in the atmosphere, and during the period of high volcanic activity it can provide a large surface for heterogeneous interactions with other atmospheric compounds. Icelandic v-dust was chosen as a case study due to frequency of volcanic eruptions and high aeolian activity in the area. In this study, we focus on the kinetics and mechanism of the reaction of sulfur dioxide (SO₂) with natural v-dust samples under atmospheric conditions using coated wall flow tube reactor and diffuse reflectance infrared Fourier transform spectroscopy (DRIFTS). Steady state uptake coefficients determined are in the range of 10⁻⁹ to 10⁻⁸ depending on the considered v-dust. Concomitantly with SO₂ uptake, both sulfites and sulfates are monitored on the surface of v-dust, with sulfates being the final oxidation product, attesting of SO₂ surface reaction. Surface hydroxyl groups play a crucial role in the conversion of SO₂ to sulfites as evidenced from both flow tube and DRIFTS experiments. Based on these experimental results, a mechanism for SO₂ interaction with different surface sites of v-dust is proposed and discussed. This study provides original insights in the kinetics of SO₂ uptake under simulated atmospheric conditions and its mechanism and transformation on volcanic material. To that regards, it brings an accurate perspective on SO₂ heterogeneous sinks in the atmosphere.

1. Introduction

Volcanic eruptions comprise one of the most significant natural hazards directly threatening people living in the proximity, and, in the

extreme case, can affect livelihoods of the humankind on the global scale. Large volcanic eruptions of the past have significantly influenced Earth's climate by injecting vast amounts of volcanic gases and aerosols into the atmosphere (Stevenson et al., 2003). Volcanic emissions can

* Corresponding author.

E-mail address: darya.urupina@imt-lille-douai.fr (D. Urupina).<https://doi.org/10.1016/j.atmosenv.2019.116942>

Received 23 April 2019; Received in revised form 26 August 2019; Accepted 28 August 2019

Available online 03 September 2019

1352-2310/ © 2019 Elsevier Ltd. All rights reserved.

cause both regional and global changes to climate by affecting monsoon circulation, causing either excessive or limited rainfall thus leading to floods and droughts (Stevenson et al., 2003), (Highwood and Stevenson, 2003), (“Tambora and the ‘Year Without a Summer’ of 1816,” 2016). Volcanic particles have an ability to affect the climate by scattering solar radiation and thus changing the Earth radiation budget (Langmann, 2013). Besides, volcanic ash, having optical and thermal properties similar to those of the black carbon, can absorb solar radiation (Arnalds et al., 2016). Vernier et al. highlighted the significance of the radiative impact of ash, in particular in the tropical latitudes due to the Brewer-Dobson circulation that sustains ash in the stratosphere for longer than was generally assumed (Vernier et al., n.d.). Finally, volcanic ash particles can affect the climate through influencing cloud formation processes and acting as ice nucleation sites during plume rise (Durant et al., 2008). The impact of v-dust on Earth's atmosphere is governed by the physical and chemical surface properties of the particles. However, the physico-chemical processes that govern the modifications of the particle surface in the plume and in the cloud when ash is in contact with volcanic gases remain poorly investigated.

Volcanic eruptions are a highly variable sources of solid particles ranging from 33 million tons (Mt) on an average year to over 100,000 Mt of ash after a major volcanic eruption, as was the case for the eruption of Mount Tambora in 1815 (Andreae, 1995). With respect to atmospheric chemistry the most significant impact would be expected to come from the particles that are in the 0.002–10 μm range as they can be carried over thousands of kilometers before eventually being deposited onto land or into the ocean by gravitational settling and wet deposition (Finlayson-Pitts and Jr, 1999), (Langmann et al., 2010), (Dagsson-Waldhauserova et al., 2014). When settled on land, v-dust (v-dust) can then be once again remobilized by the wind and entrained into the atmosphere. Some places on Earth are particularly prone to high aeolian activity. Such is, for example, the case for Iceland, that experiences on average about 135 dust days per year, partly due to frequent volcanic eruptions and re-suspension of volcanic materials (Dagsson-Waldhauserova et al., 2014). In fact, this volcanic island of North Atlantic with an area of 103,000 km^2 lying south of the Arctic Circle is one of the dustiest areas of the world as well as the largest desert in Europe and the Arctic (Dagsson-Waldhauserova et al., 2014). It is also one of the most volcanically active areas. There are about 30 active volcanic systems and volcanic eruptions occurring every 3–5 years on average (Thordarson and Larsen, 2007), (Schmidt et al., 2014). Frequent dust events in Iceland transport dust over long distances, often exceeding 2500 km, towards High Arctic (> 80° N) and Europe (Ovadnevaite et al., 2009), (Groot Zwaaftink et al., 2017), (Moroni et al., 2018), (Dordevic et al., 2019). Located only 1000 km from mainland Europe, it makes a particularly interesting case study due to its proximity to densely populated European countries.

In the stratosphere, emissions of volcanic ash were linked to ozone reduction recorded after major volcanic eruptions, such as El Chichón eruption in Mexico in 1982 and Mount Pinatubo eruption in Philippines in 1991 (Brasseur et al., 1990), (“Reactions on Mineral Dust - Chemical Reviews (ACS Publications),” n.d.). Even if the effect of volcanic ash in the chemistry of the troposphere has not yet been evaluated, it is suggested that ash particles act as a long-range transporting carrier for various species adsorbed on their surface and as a solid support for their reactions with atmospheric trace gases (Li et al., 2006), (Maters et al., 2017). Some of these species are formed during eruption, when a variety of gases are released along with volcanic ash. Sulfur dioxide (SO_2) is typically the third most emitted volcanic gas after water and carbon dioxide (Durant et al., 2010). SO_2 is known to contribute to the formation of sulfuric acid aerosol, which, when injected in the stratosphere, stays there for up to 2 years effectively cooling the troposphere below (Stevenson et al., 2003), (Highwood and Stevenson, 2003).

Volcanic ash and SO_2 are likely to participate in a variety of heterogeneous reactions that could potentially influence the balance of other atmospheric species. SO_2 has already been shown to exhibit

heterogeneous reactivity towards many mineral oxides such as MgO , Al_2O_3 , Fe_2O_3 and TiO_2 (Usher et al., 2002). Along SO_2 uptake on these materials, sulfite and sulfate formation was detected on the surface of most mineral oxides and synthetic mineral dust and it was proposed that hydroxyl groups and surface-active oxygen are responsible for oxidation of sulfites to sulfates (Zhang et al., 2006). Nevertheless, limited data exist on the mechanism of the interaction of SO_2 gas with natural multi-component samples, such as volcanic ash as well as on the stability of the surface species formed during reaction.

It was recently evidenced by Maters et al. that volcanic ash is reactive to the uptake of weakly acidic SO_2 gas with a reactivity that is proportional to the abundance of strongly basic sites, such as those affiliated with alkaline and alkaline earth metals (Maters et al., 2017). Although very informative of the processes occurring on the short scale, the initial uptake and the total uptake capacity measured by the authors have limited ability to explain the interactions on the longer time scale. Besides, the above-mentioned experiments were performed in a Knudsen cell under very low pressure and dry conditions that are not compliant with the atmospheric processes (Maters et al., 2017). It was therefore decided to undertake a comprehensive study of the interactions of SO_2 with v-dust under atmospheric conditions. Iceland was chosen as a location of interest for sample collection required to study heterogeneous reactivity of volcanic ash and SO_2 gas. The scope of this study is threefold. First, different natural volcanic and Icelandic samples were collected and characterized using various techniques, such as SEM (Scanning Electron Microscopy) and ICP-MS (Inductively Coupled Plasma-Mass Spectrometry). Second, the uptake of atmospheric SO_2 by the surface of selected v-dusts was investigated using a flow tube reactor. Finally, Diffuse Reflectance Fourier Transformed Spectroscopy (DRIFTS) employed for the *in-situ* monitoring of adsorbed phase was used to identify the surface species formed and to clarify the surface reaction mechanisms. The *in-situ* spectroscopic approach has been complemented by HPLC (High-Performance Liquid Chromatography) technique employed for quantification of the surface products.

2. Experimental section

2.1. Materials

2.1.1. Origin of the dust samples

All five samples of v-dust come from different dust hot spots of Iceland. The properties of Hagavatn (64°28'6,12"N 20°16'55,81"W), Mýrdalssandur (63°26'50.1"N 18°48'52.8"W), Maelifellssandur (63°48'48.7"N 19°07'42.5"W) and Dyngjúsandur (64°50'41,885"N 16°59'40,78"W) v-dusts are described by Arnalds et al. (2016). Overall, these areas are subjected to extremely large aeolian erosion due to frequent dust storms, and have extensive areas (10–140 km^2), hence providing a large supply (31–40 million tons annually) of v-dust to the atmosphere. Samples were collected from the top surface layer of each dust hot spot. The samples were dry and did not come in contact with soil or other organics. The fifth sample of Eyjafjallajökull (63°33'50.4"N 19°27'28.8"W) volcanic ash was collected and stored dry during the second phase of the explosive-effusive volcanic eruption on April 27. It is a typical volcanic ash sample as characterized by Gíslason et al. (2011).

2.1.2. Characterization of the samples

Scanning Electron Microscopy/Morphology of the samples was analyzed by SEM carried out on a Hitachi S-4300SE/N SEM in high vacuum mode. The images of different v-dust particles are presented in Fig. 1. These are small particles with rough edges. Dust from Eyjafjallajökull (Fig. 1e) has larger particle size with many particles reaching 500 μm in diameter, while the other four dusts (Fig. 1a–d) have a much finer structure and range from 10 to 50 μm in diameter due to glaciofluvial processes leading to their generation.

Specific surface area measurements/To avoid any overestimation

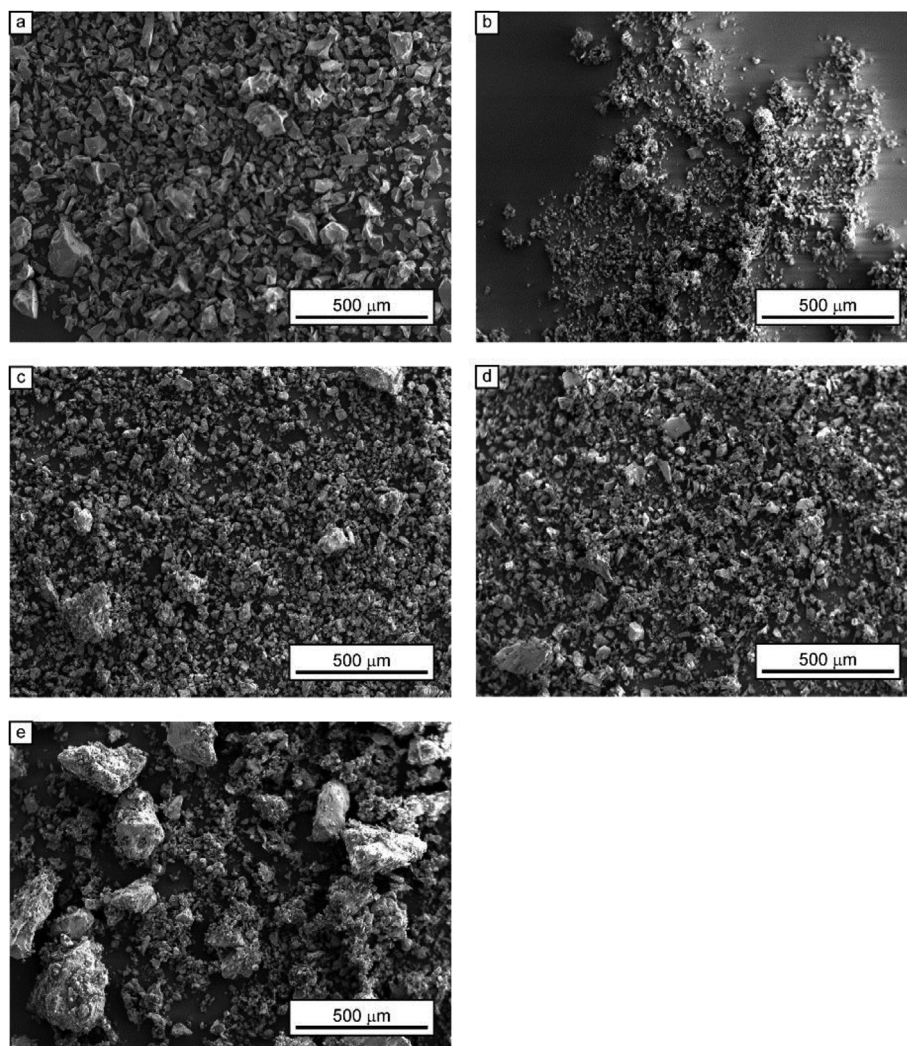


Fig. 1. SEM images of five v-dusts: (a) Mýrdalssandur, (b) Dyngjusandur, (c) Hagavatn, (d) Maelifellsandur, (e) Eyjafjallajökull.

of the uptake coefficients by the use of the geometric surface of the sample bed, it was decided to use the specific surface area (SSA) in the uptake calculations as discussed in the latest IUPAC evaluation (Crowley et al., 2010). In brief, the determination of the uptake coefficient using the geometric surface - i.e. the geometric area of the tube covered with the volcanic dust as noted in equation (2) (see section 2.2.1) of the manuscript-overestimates the uptake since it does not consider all the surface of the dust as accessible to gaseous SO_2 . However, in a series of experiments it was evidenced that the entire surface area of the sample is accessible to the gas environment and thus the total surface area of the dust deposited in the tube should be used to determine the real uptake coefficient. The SSA is a physical property of solids, which represents the total surface area of a material per mass unit ($\text{m}^2 \text{g}^{-1}$), and is used for the determination of the kinetic and sorption parameters (see section 2.2.1). To determine SSA, the Brunauer–Emmett–Teller (BET) method was employed. Nitrogen (N_2) adsorption measurements were performed with a laboratory gas sorption analysis system (Joshi et al., 2017), (Ibrahim et al., 2018) within 0.05–0.3 relative pressure range (P/P_0) of N_2 . To determine the range of uncertainty, three adsorption measurements were conducted for each sample. The results of the BET specific surface area (SSA_{BET}) of the 5 samples are displayed in Table 1.

Chemical composition/The bulk elemental composition of the samples of Icelandic v-dust used in this study was determined by ICP-MS using a Perkin Elmer NeXion 300x spectrometer, the results are

Table 1

BET Specific Surface Area of the v-dust samples used in this study.

Origin of the Icelandic v-dust sample	BET Specific Surface Area ($\text{m}^2 \text{g}^{-1}$)
Mýrdalssandur	1.5 ± 0.38
Dyngjusandur	7.0 ± 1.8
Hagavatn	4.5 ± 1.1
Maelifellsandur	8.2 ± 2.0
Eyjafjallajökull	0.75 ± 0.19

presented in Table 2. Prior to the analysis, from 2 to 7 mg of each sample were treated in a mixture of acids ($\text{HF}/\text{HNO}_3/\text{H}_2\text{O}_2$) in a microwave oven (Milestone Ultrawave) at 500 K and 35 bar for 15 min (Alleman et al., 2010). Six measurements per sample were performed to evaluate their chemical heterogeneity. Repeated measurements were carried out on acid blanks, quality control standard solutions and standard reference material (NIST SRM 1648a and SRM 2584) to evaluate detection limits, accuracy and to validate the whole procedure. As can be seen from Table 2 silicon is the most abundant element of the v-dust, followed by iron, calcium, and aluminum. Within the five selected v-dust samples the elemental composition seems to differ only slightly, except for Eyjafjallajökull v-dust which exhibits a higher amount of silicon than other samples and a lower amount of calcium, iron and magnesium. The results of ICP-MS analysis for Eyjafjallajökull v-dust agrees well with the literature (Gislason et al., 2011). The

Table 2

% Elemental composition of the v-dust samples used in this study and of mineral dust samples adopted from (Joshi et al., 2017), as determined by ICP-MS experiments.

Element	Mýrdalssandur	Dyngjusandur	Hagavatn	Maelifellssandur	Eyjafjallajökull	Bordj Saharan dust (Joshi et al., 2017)	Gobi dust (Joshi et al., 2017)
Si	31.3 ± 2.2	32.7 ± 2.0	27.5 ± 2.8	28.3 ± 2.4	49.5 ± 0.9	94.4	57.6
Fe	23.0 ± 1.5	19.7 ± 0.2	19.6 ± 0.7	23.8 ± 0.8	13.0 ± 0.5	1.3	5.5
Ca	13.9 ± 1.3	16.3 ± 0.3	19.5 ± 1.1	14.0 ± 0.3	7.3 ± 0.1	1.0	16.1
Al	12.3 ± 3.1	15.8 ± 0.2	16.7 ± 3.2	15.5 ± 0.1	13.6 ± 0.9	1.8	11
Mg	5.1 ± 1.2	7.3 ± 0.1	10.4 ± 1.8	5.7 ± 0.4	3.3 ± 0.2	0.1	2.3
Ti	7.6 ± 0.7	3.3 ± 0.4	2.4 ± 0.1	6.1 ± 0.4	2.4 ± 0.1	0.7	0.8
Na	4.8 ± 0.2	3.9 ± 0.1	3.1 ± 0.1	4.6 ± 0.1	7.3 ± 0.3	0.2	2.5
K	1.3 ± 0.2	0.6 ± 0.1	0.2 ± 0.1	1.5 ± 0.1	3.1 ± 0.1	0.1	3.5
other	0.7	0.4	0.6	0.5	0.5	0.1	0.7

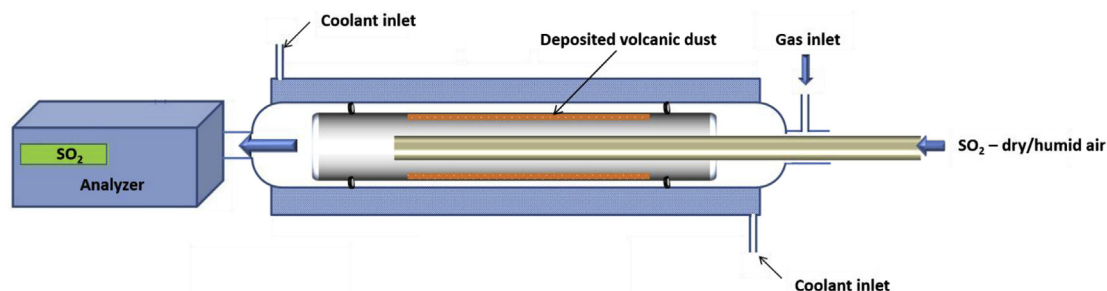


Fig. 2. Schematic representation of the Coated wall Flow Tube (CWFT) reactor used in this study. The space filled with the coolant in between the two walls is shaded in blue. The dust sample coating the inner surface of the Pyrex tube is shown in orange. (For interpretation of the references to color in this figure legend, the reader is referred to the Web version of this article.)

difference in the composition of Eyjafjallajökull v-dust in comparison with other samples is most probably due to the difference in the composition of magma that produced it. Indeed, the volcanic systems that supply Dyngjusandur dust hotspot (Bárðarbunga and Kverkfjöll volcanic systems) and Mýrdalssandur and Maelifellssandur dust hotspots (Katla volcanic system) have magmas of a predominantly basaltic composition, while magma of Eyjafjallajökull is andesitic, meaning that it is higher in silicon (“Icelandic Volcanoes,” n.d.), (Vogel et al., 2017). The decrease of calcium, iron and magnesium with increasing silicon content is in accordance with the expected variation of the composition of magma (Vogel et al., 2017). Other processes that can influence the composition of magma during a particular eruption include crystallization (Clague and Denlinger, 1994), melting of the crustal rocks (Deegan, 2010) and mixing of original magma with another magma that evolved separately (“Icelandic Volcanoes,” n.d.). Since composition of magma can change within the same eruption, one might expect to see different compositions of v-dust both on the time scale and on the location scale. Transported dust can also have a different composition further away from the source. Globally, when compared to other types of mineral dusts, such as Saharan dusts or Gobi dust (Joshi et al., 2017), the amount of silicon in all five v-dust samples is considerably lower while the amount of iron, magnesium, and titanium is higher (Romanias et al., 2016), (Langmann, 2013).

2.1.3. Gases

Experiments are carried out using zero air; it is generated by a classical air compressor, and then passed through a catalytic zero air generator (Claind ZeroAir, 2020, Lenno, Italy) coupled to a swing adsorption (PSA) device. The remaining impurity levels in the air stream before entering the reactor are lower than the analytical system detection limits: VOCs < 0.1 ppb, CO₂ < 10 ppb, and CO < 80 ppb. Moisture level is ca. 2 ppm. In experiments requiring humid air, a second flow of zero air going through a bubbler of ultrapure water (milli-Q, resistivity 18.2 MΩ cm) is mixed with the dry air flow, in proportions necessary to reach the relative humidity (RH) targeted. Certified gas cylinders are used as SO₂ source. For low concentration

experiments aiming to determine uptake coefficients in the flow tube, an SO₂ cylinder of 8.96 ppm in air (20.7% O₂, 79.3% N₂) provided by “Air Liquide” is used. Regarding the mechanistic investigation employing DRIFT spectroscopy, higher concentrations are used and a certified cylinder of 250 ppm (Messer, France) diluted in synthetic air (nearly 80% N₂ and 20% O₂) is the SO₂ source.

Throughout the manuscript, gas concentrations are given in ppmv and ppbv (parts per million and parts per billion by volume, respectively). Under usual experimental conditions ($T = 296\text{ K}$, $P = 1\text{ atm}$), the conversion to a concentration is given by 1 ppbv (SO₂) $\approx 2.5 \times 10^{10}$ molecules cm⁻³. Note that this conversion factor takes a different value when the temperature or total pressure changes.

2.2. Experimental set ups

2.2.1. Coated wall flow tube reactor

The heterogeneous interaction of SO₂ with v-dust was investigated in a horizontal double wall flow tube reactor represented schematically in Fig. 2. The experiments were conducted under relevant atmospheric conditions, i.e. SO₂ concentration in the ppb range, atmospheric pressure, room temperature, under dry conditions and 30% RH. The objective of this series of experiments was to determine the uptake coefficients of SO₂ on the various Icelandic v-dusts.

The setup was described in detail in a previous paper (Lasne et al., 2018) it mainly consists of three parts; (i) the gas mixing line, (ii) the reactor and (iii) the analytical device. The gas preparation line is used for the mixing of zero dry/humid air with SO₂ resulting in a flow with the desired proportion of RH and SO₂ concentration. The reactor is made of a double wall Pyrex glass and is thermostated by circulating water in between the double wall surrounding the flow tube. Inside and along the axis of the reactor, a Pyrex tube covered on its inner wall with the v-dust is introduced. To coat the inner surface of a Pyrex tube with v-dust (orange color in Fig. 2), a defined mass of dust is first inserted in a tube. A small amount of water is added to form a slurry and the tube is shaken to deposit an even coating on the Pyrex surface. Then, the tube is heated slightly above 380 K for 10 min to evaporate excess water,

placed in the reactor and flushed overnight with dry air. Potential modifications of the volcanic dust upon its dissolution in water in the process of slurry preparation and subsequent drying process include displacement of soluble salts that might be found on the surface of v-dust particles as well as leaching of alkali and alkaline earth metals from the aluminosilicate network at ash surfaces (Witham et al., 2005). In the case of Hagavatn, Mýrdalssandur, Maelifellssandur and Dyngju-sandur natural v-dust samples, that were likely previously exposed to water the above mentioned phenomena does not seem to effect the results because the soluble salts would be expected to leach out by the time of the experiment. In the case of fresh Eyjafjallajökull dust leaching of the soluble salts formed during ash-gas interaction in the plume presents a valid concern. In order to minimize removal of soluble salts the amount of water added to prepare a slurry was as small as necessary to spread the dust evenly, i.e. in the case of Eyjafjallajökull 1:3 ash (g) to water (mL) ratio was used, which is much smaller than the 1:25 ash-to-water ratio recommended for preparation of ash leachates (Witham et al., 2005). In addition, contact time with water was minimized to around 10 s shaking followed by rapidly drying the slurry, which is also much faster than 90 min agitation procedure recommended by Witham et al. (2005). One could also expect that drying the slurry would lead to redistribution of the displaced salts, even though some of it could be redeposited on the surface of the glass tube and not the v-particles. Two Viton O-rings are placed around the Pyrex tube to fix its position inside of the reactor. The gas mixture is flowed through a movable injector (internal diameter of 0.3 cm) with a flow rate ranging between 250 and 500 sccm, ensuring laminar flow conditions with a Reynolds number, $Re < 50$. The role of the moveable injector is to either isolate (placed at the downstream end of the flow tube) or to expose the dust surface to the gas environment (upstream end of the reactor). The outgoing flow is then directed to the SO₂ analyzer (Model 43C, Thermo Environmental Instruments Inc.) for the real time gas phase monitoring of SO₂, with a time resolution of 10 s. We didn't noticed any loss of dust during the uptake experiments. Note that the tubes with the deposited dust are weighted before and after the experiments and the variations noticed were in the range of the mass scale uncertainty (< 1%). In addition, considering that the flow rate during the experiments is relative slow, the experiments are carried out under atmospheric pressure and no pressure variation takes place between the reactor and the analyzer, it is highly improbable to experience any loss of dust during our measurements. Furthermore, we have not observed (at least visually) any large particles to fail to adhere to the Pyrex tube. However, even if this was the case, in the horizontal flow tube, these particles would still be subjected to the flow of gas and thus remain accessible to the gas. To conclude, the total mass of the dust inside the reactor is maintained during the entire experiment and is accessible to the gas environment and hence the total surface area does not change and no correction is required to determine the uptake coefficients. The uptake of SO₂ by v-dust is studied under dark conditions at $T = 296$ K, $[SO_2] \approx 75$ ppb (1.88×10^{12} molecules cm⁻³) in air, and a relative humidity of either 30% or under dry conditions (i.e. $RH < 0.1\%$). Regarding RH , studying the uptake under dry conditions provides an evaluation of the interaction of the probe gas with the direct surface of volcanic material, while increasing RH to 30% contributes to the understanding of the impact of the water coverage on the mineral aerosol (Joshi et al., 2017).

Theoretical SO₂ concentration profile is represented in Fig. 3. During a typical flow tube experiment SO₂ is flowed through the reactor, the dust being left unexposed initially. After a stable SO₂ concentration, $[SO_2]_0$, is set, the injector is pulled out and the dust is exposed to SO₂; the change in SO₂ concentration related to its uptake by dust is recorded by the SO₂ analyzer. After a steady-state is reached, the injector is pushed back in to control the $[SO_2]_0$. What is obtained as a result of the flow tube experiment is a time evolution of the trace gas concentration at the tube exit, the so-called breakthrough curve, that is used to calculate the steady state uptake coefficient (Huthwelker et al.,

2006). In the case of SO₂ a long-lasting tailing of the breakthrough curve is observed, similar to the one described for the uptake of nitric acid (HNO₃) on ice (Huthwelker et al., 2006). This phenomena leads to the following question: at which point can we say that a steady state is reached? In the absence of the generally accepted understanding of the nature of tailing and for the practical reasons the following pragmatic approach was adopted. Steady state is considered to be reached when the variation of the signal falls within 1.5% of its value for at least 3 h. On average it takes about 12 h to reach the steady state under 30% humidity, which is much longer than 1 h needed to achieve a steady-state for the uptake of ozone by clay dust (Lasne et al., 2018).

Preliminary experiments were conducted to determine a possible contribution of the Pyrex surfaces to the uptake of SO₂. They showed negligible contribution to the parameters determined in the current study.

The measurements of $[SO_2]$ at steady-state and at the initial level, $[SO_2]_0$, together with the knowledge of the parameters defining our setup are necessary to conduct the analysis leading to the determination of the uptake coefficients under equilibrium conditions, γ_{ss} (Lasne et al., 2018). Assuming first order kinetics for the uptake of SO₂ by v-dust surfaces, the observed constant of reaction, k_{obs} (in s⁻¹), is determined by (1):

$$k_{obs} = \frac{v}{L} \times \ln\left(\frac{[SO_2]_0}{[SO_2]}\right) \quad (1)$$

where v is the flow in the reactor (in cm s⁻¹) and L is the length of the dust coating (in cm). The value of k_{obs} (in s⁻¹) is corrected for diffusion of SO₂ with a constant k_{diff} (in s⁻¹) to give the diffusion-corrected constant k_{kin} (in s⁻¹). In this work, a diffusion coefficient of SO₂ in the air derived from (Massman, 1998) is used, $D(296$ K) = 95.28 Torr cm² s⁻¹. This value is in excellent agreement with $D = 94 \pm 13$ Torr cm² s⁻¹ suggested by Tang et al. (2014). The diffusion-corrected constant, k_{kin} , is then used to determine γ_{ss} , (2):

$$\gamma_{ss} = \frac{4k_{kin}V}{cS_{geom}} \quad (2)$$

where V and S_{geom} are the volume (in cm³) and geometric surface (in cm²) of the region where the reaction takes place, respectively, and c is the average molecular speed (in cm s⁻¹). The diffusion-correction accounts for ca. 5% of the measured uptake coefficients.

A series of experiments were carried out as a function of Mýrdalssandur v-dust mass deposited that showed a linear increase in the 0–250 mg range. The linear increase of the uptake with mass and the lack of saturation reflect the fact that the entire surface of the dust is accessible to SO₂ molecules from the gas and thus the specific surface area SSA_{BET} is used for the calculation of the uptake coefficient, $\gamma_{ss,BET}$, (3):

$$\gamma_{ss,BET} = \gamma_{ss} \times \frac{S_{geom}}{A_s} \quad (3)$$

where A_s is the effective surface area of the dust, obtained from multiplying SSA_{BET} (m² g⁻¹) by the mass of the sample (g).

The error on the uptake coefficients is the root-mean-square deviation of the values measured. It was calculated with the precision of the signal (0.5% of the measured concentration) and its propagation to k_{obs} measurement, the SSA determination (~25%) and all relevant uncertainties, i.e. on the gas flow measurement, temperature, mass weighting, and length of the exposed dust coating (~8%). The total error calculated for the γ values was estimated to be ca 35% in all experiments and a safe limit of 40% is given. Although the quoted uncertainty is significant, it reflects the real error accounted for the measurement of slow uptake processes (uptakes on the order of 10⁻⁹) in the flow tube.

Besides uptake coefficients, the transient initial number of SO₂ molecules taken up per surface area of v-dusts N_t (molecules cm⁻²) is determined at 30% of RH ; by integrating the area of the initial uptake

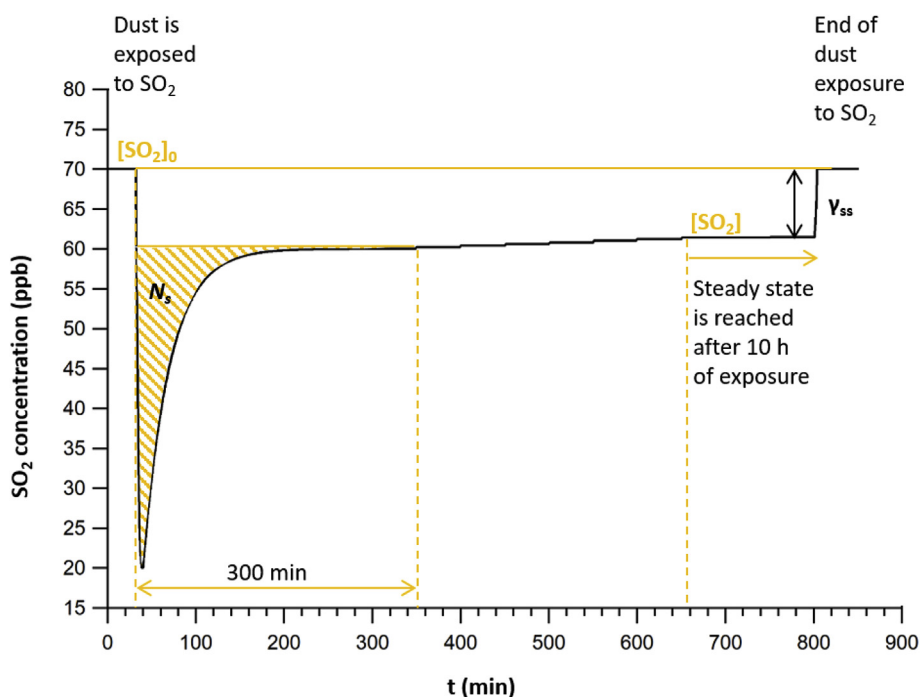


Fig. 3. Theoretical SO_2 concentration profile during a typical flow tube experiment with v-dust exposed to SO_2 . At the beginning of the experiment where surface is isolated from the gas mixture the initial SO_2 concentration is $[\text{SO}_2]_0$, then the dust is exposed to the gas and the concentration of SO_2 falls to its minimum, after which it recovers till a steady-state is reached. Note that the steady-state concentration $[\text{SO}_2]$ is different from the initial state concentration $[\text{SO}_2]_0$. Initial concentration is controlled when the injector is pushed in and the SO_2 gas is no longer in contact with the dust. Shaded area corresponds to the integrated area that is used to obtain the number of molecules during the transient initial uptake of SO_2 on v-dusts N_s (molecules cm^{-2}). 300 min was chosen as integration limits for the determination of N_s .

process in a typical uptake experiment (Fig. 3) divided by the effective surface area of the dust, A_s , according to (4):

$$N_s = \int_{\tau=0}^{\tau=t} \frac{F_t}{A_s} d\tau \quad (4)$$

where F_t is the flow rate (molecules min^{-1}) of SO_2 molecules through the reactor. The total error in N_s determination is estimated to be ca. 30% and includes all systematic uncertainties and the error in SSA determination.

It should be noted that since the SO_2 concentration recorded at the steady-state was lower than its pre-exposure concentration, for the determination of N_s solely the transient initial uptake removal of SO_2 is considered (dashed area in Fig. 3). The long tailing of the breakthrough curve observed points to additional physico-chemical processes besides the absorption/desorption. Therefore for the determination of integration parameter a similar to two-third criterion approach was adopted as recommended by Huthwelker et al., where “the surface uptake is considered finished once the breakthrough curve rises to two-thirds of its initial value” (Huthwelker et al., 2006). The integration limits for the determination of the number of molecules N_s were chosen from the time of the exposure of SO_2 to the dust to 300 min after the exposure to make sure that the change in the breakthrough curve towards steady state has occurred for all the dusts. This criterion was adopted in order to be able to compare the uptake capacity of the v-dusts at the initial stage of the interaction with SO_2 . On longer scale, samples can be compared based on the $\gamma_{ss,BET}$ values.

2.2.2. DRIFTS experiments

The heterogeneous interaction between SO_2 gas and v-dusts was studied *in-situ* inside of the optical DRIFTS cell operated at atmospheric pressure and room temperature under dry and 30% RH conditions. The objective of this series of experiments was to monitor the adsorbed species formed on the surface of v-dusts, aiming to elucidate the mechanism of the interaction under both dry and humid conditions.

The DRIFT experimental setup consists of three parts: (i) the gas supply line, (ii) the optical reactor, and (iii) the analytical device as described previously by Romanias et al. (Romanias et al., 2016). A representation of the system is given in Fig. 4. The heterogeneous reactions between SO_2 and different v-dust samples are monitored *in situ*

inside of the optical DRIFTS cell (Praying Mantis Kit, Harrick Scientific Corp.) fitted with zinc selenide (ZnSe) windows. DRIFT spectra are recorded by a Nicolet 6700 FTIR spectrometer equipped with a mercury cadmium telluride (MCT) detector cooled with liquid nitrogen.

The temperature of the sample is measured using a thermocouple placed right below of the sample holder and is monitored/controlled with a Harrick temperature controller (Pleasantville, USA).

At the beginning of the experiment the crucible sample holder inside the DRIFTS cell is filled with about 80–110 mg of v-dust. The cell is then tightly closed and the infrared beam is focused on the surface of the dust. The gas flowed through the DRIFTS cell is made up of different proportions of dry air, humid air and SO_2 gas. Prior to the introduction of the SO_2 gas volcanic samples are heated to 423 K for 1.5 h to remove any pre-adsorbed species. Samples are then allowed to cool down to room temperature and are purged overnight with either dry or humid air depending on the experimental conditions in order to equilibrate system. A background spectrum is recorded right before introduction of SO_2 gas. DRIFT spectra of the v-dust in the presence of SO_2 gas are recorded from 650 to 4000 cm^{-1} using Omnic software with 100 scans per spectrum, a spectral resolution of 4 cm^{-1} , and a time resolution ranging from 3 min to 1 h depending on the stage of the experiment. The formation and loss of surface species are observed as positive and negative absorption bands respectively. Thus, a typical experiment lasts about 4 days and consists of thermal pre-treatment (1.5 h), system equilibration (16 h), SO_2 adsorption phase (72 h) and desorption upon flushing phase (6 h). The SO_2 concentration in the mixed gas is 175 ppm. Note that this is over three orders of magnitude higher than the atmospherically relevant SO_2 concentration of ~ 75 ppb used in the flow-tube reactor experiments. Large difference in SO_2 concentrations used for flow tube versus DRIFTS experiments comes from different technical constrains. For instance, DRIFT spectroscopy is used for the *in situ* characterization of surface adsorbed species but is characterized by a relatively low sensitivity, depending on the gas-surface interactions. Likewise, the observation of the steady state in flow tubes, when the flowing gas is in ppm level, is not possible. In this work two different reactors serve two different purposes: flow tube is used to study kinetics by providing uptake coefficients under atmospherically relevant conditions while DRIFTS is used to study surface reaction mechanism. It is important to keep in mind that while the kinetics is changed by the

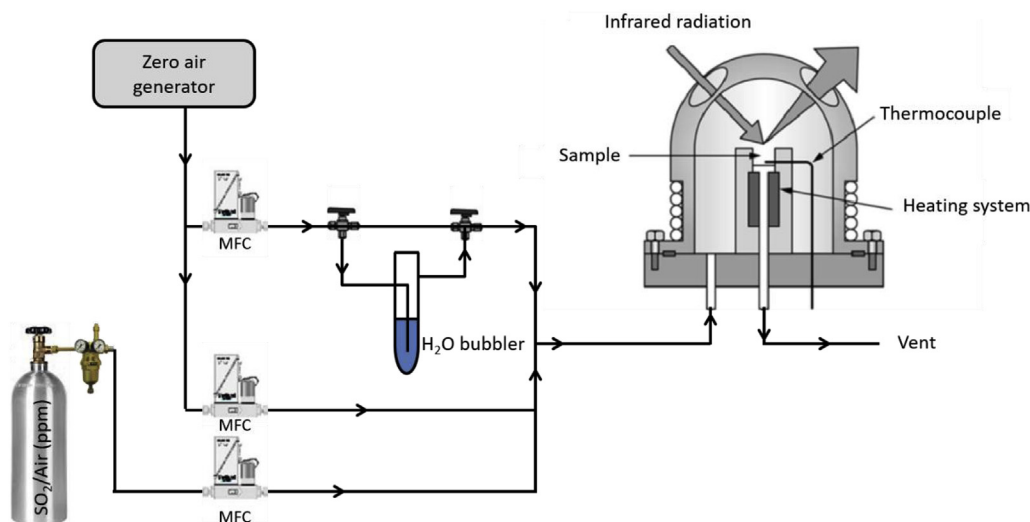


Fig. 4. Scheme of the DRIFT experimental setup. MFC: Mass Flow Controllers are used to supply the optical cell with a defined mixing ratio of dry air, humid air, and SO_2 .

concentration because the surface coverage is changed by the concentration, the reaction mechanism is not likely to be changed as a function of gas phase concentration. Thus, both techniques bring complimentary and valuable information.

2.2.3. Ion analysis

A reverse-phase HPLC method with indirect photometric detection for the simultaneous determination of sulfates and sulfites was used for quantification of sulfates and sulfites formed following experiments with DRIFTS. To prevent oxidation of sulfites to sulfates, 1.0 mL of 1% formalin in pure water is used as an extracting solvent as recommended by Michigami (Michigami and Ueda, 1994). After 20 min of mechanical shaking the extracted solution is passed through a $0.2\ \mu\text{m}$ PTFE membrane and a filtered leaching solution is analyzed by Waters HPLC system. Chromatography equipment consists of Waters 2695 Series HPLC System equipped with 2487 UV/VIS Dual wavelength absorbance detector, (Waters Corporation, Milford, MA). Empower 2 Data Acquisition System for LC (Copyright, 2005, Waters Corporation, Milford, MA) is used to analyze the data. Analysis is performed using Restek Ultra Column C18, $5\ \mu\text{m}$, Length 250 mm, I.D. 4.60 mm column dynamically coated with 1.0 mM cetylpyridinium chloride in 7% acetonitrile solution to produce a charged surface as recommended by Zuo et al. (Zuo and Chen, 2003) The HPLC instrument is operated isocratically at ambient temperature using Methanol-Potassium Hydrogen Phthalate Buffer 1.0 mM, adjusted to pH 6.5 with dilute potassium hydroxide (1:99, v/v) mobile phase and run at a flow rate of 1 mL/min for 15 min. The injection volume is $10\ \mu\text{L}$. Detector is set at 255 nm. All chemicals and solvents used for HPLC analysis are of analytical grade.

3. Results and discussion

3.1. Exploring SO_2 uptake on v-dust from the gas phase: flow tube study

3.1.1. First insight on SO_2 uptake on various natural v-dusts under ambient conditions

The uptake of atmospheric relevant concentration of SO_2 (i.e. $\approx 75\ \text{ppb}$) by the surface of five selected v-dusts under typical atmospheric conditions of ambient temperature, pressure and 30% RH was investigated using the flow tube reactor (Lasne et al., 2018). A typical uptake profile depicted in Fig. 5 shows the $[\text{SO}_2]$ uptake of Mýrdalssandur dust in humid ($\text{RH} = 30\%$) conditions. It is clearly observed from the profile that after the initial uptake of the gas upon exposure of the v-dust the system reaches a steady-state $[\text{SO}_2]$ that is

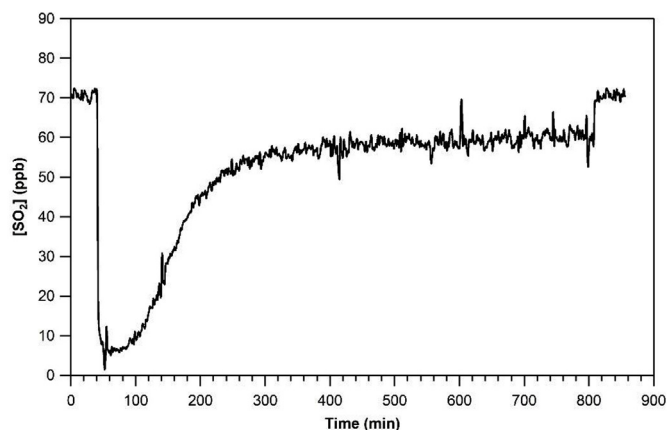


Fig. 5. SO_2 concentration recorded by the analyzer during exposure of Mýrdalssandur v-dust at $T = 296\ \text{K}$, $\text{RH} = 30\%$.

distinct from the initial state $[\text{SO}_2]_0$, evidencing continuous consumption of the title molecule at least for the duration of the experiment. All the samples under investigation demonstrated both an initial uptake and a steady state uptake (similar to Fig. 5). The latter is worth investigating as it suggests the ability of the v-dusts to exhibit a long-term effect on the equilibrium composition of the atmosphere. The steady state coefficients are in the order of 10^{-9} to 10^{-8} (Fig. 6, Table 3). These values are much lower than the values obtained by Maters et al., who reported the initial uptakes of SO_2 on volcanic ash and glass powders at 10^{-3} to 10^{-2} range (Maters et al., 2017). Large difference in values is not surprising though for a number of reasons. First, the initial uptake describes an uptake on the fresh surface at the first instances of its interaction with gas, while the steady state uptake is an ongoing phenomenon reflecting the ability of the surface to adsorb gas continuously. Second, while determining initial uptakes geometric surface area was used by Maters et al. in order to calculate uptake coefficient (Maters et al., 2017), while specific surface area was used in this study in order to account for all the surface accessible to the SO_2 molecules on longer time scales. Using geometric vs specific surface area gives an upper value for the uptake coefficient (Crowley et al., 2010). Finally, in the study of Maters et al. experiments were performed under dry conditions contrary to 30% RH used in this study. Moreover, in the adsorption/desorption experiments on the volcanic glasses performed by Schmauss and Keppler it was observed that the first layer of

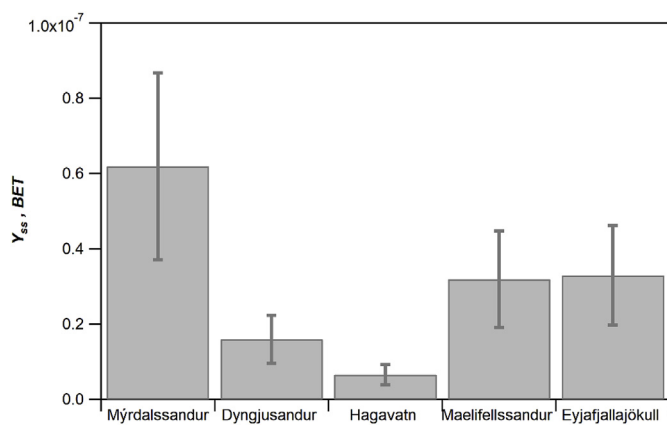


Fig. 6. Steady-state uptake coefficients of the Icelandic v-dust samples at $[\text{SO}_2]_0 \approx 75$ ppb, $\text{RH} = 30\%$, $T = 296$ K, under dark conditions. The errors quoted reflects the total error for the steady state uptake coefficient determination.

Table 3

SO_2 steady-state uptake coefficients ($\gamma_{\text{ss,BET}}$) and transient initial number of molecules adsorbed (N_s) on the surface of v-dusts. Experimental conditions: $[\text{SO}_2]_0 \approx 75$ ppb, $\text{RH} = 30\%$, $T = 296$ K, under dark conditions.

Origin of the Icelandic v-dust	$\gamma_{\text{ss,BET}}$	N_s (molecules cm^{-2})
Mýrdalssandur	$(6.2 \pm 2.5) \times 10^{-8}$	$(2.5 \pm 0.8) \times 10^{13}$
Dyngjusandur	$(1.6 \pm 0.6) \times 10^{-8}$	$(2.1 \pm 0.6) \times 10^{13}$
Hagavatn	$(6.6 \pm 2.6) \times 10^{-9}$	$(1.2 \pm 0.4) \times 10^{13}$
Maelifellssandur	$(3.2 \pm 1.3) \times 10^{-8}$	$(9.6 \pm 2.9) \times 10^{12}$
Eyjafjallajökull	$(3.3 \pm 1.3) \times 10^{-8}$	$(1.2 \pm 0.4) \times 10^{13}$

SO_2 molecules was adsorbed on the surface of volcanic glass irreversibly and could not be removed (Schmauss and Keppler, 2014).

Interestingly, the obtained results show somewhat contrasted behaviors from one sample to another. In the literature the differences in the uptake of SO_2 on solid material are commonly linked to the differences in elemental composition or mineralogy (Maters et al., 2017), (Maters et al., 2016), (Usher et al., 2002), (Zhang et al., 2006), (Harris et al., 2012). Using synthetic and natural silicate glasses as proxies for fresh unweathered volcanic ash is commonly done due to the fact that glass often represents a major component of v-dust. Besides, a thin layer of glass covering the crystalline components of ash surfaces was observed (Delmelle et al., 2018). Several studies indicated that sulfates are more likely to get adsorbed on the glass fraction of volcanic dust (Schmauss and Keppler, 2014), (Farges et al., 2009). While investigating trends in adsorption of SO_2 on glass, elemental composition is commonly investigated (Maters et al., 2017). This approach though ignores the crystalline phase of the volcanic dust. Maters et al. emphasized that the influence of crystallinity on the adsorption of SO_2 gas is not yet understood (Maters et al., 2017). On the other hand author working with natural mineral dust samples, such as desert dusts often approximate composition of dusts using simple mineral oxides and look for trends in adsorption in relationship with the mineral phase composition. In our study v-dusts differ significantly in their crystalline fraction. Volcanic samples used in this study contain from 20% (Hagavatn) to 80–90% (Mýrdalssandur, Maelifellssandur and Dyngjusandur) of amorphous material (Baratoux et al., 2011), (Moroni et al., 2018). The remaining part is crystalline. Eyjafjallajökull is also dominated by glass (Gislason et al., 2011). Plagioclase, pyroxene, and olivine are the mineral phases reported in all five samples, while magnetite was only found in Mýrdalssandur and Maelifellssandur (Moroni et al., 2018), (Baratoux et al., 2011) (Gislason et al., 2011). A very small amount of crystalline silica was found in Eyjafjallajökull and none was reported for other samples (Gislason et al., 2011).

Since amorphous fraction dominates composition of v-dusts, an attempt to find trends in the uptake vs elemental composition was undertaken. Among the authors linking the differences in uptake coefficient to the elemental composition Maters et al. observed increase of the initial uptake of SO_2 on the surface of synthetic volcanic glasses with decrease of their silica (Si) content and increase of the sum of their sodium (Na), potassium (K), magnesium (Mg) and calcium (Ca) content (Maters et al., 2017). As for the natural volcanic samples the relationship was not as straightforward, even though a dependence of the initial uptake on the total surface content of the sum of Na, K, Mg and Ca was suggested (Maters et al., 2017). In our studies no clear correlation between the bulk elemental composition of a v-dust and its uptake of SO_2 was established. It can be due to the fact that the elemental concentration in the bulk sample may not represent the availability of the elements on the surface. Therefore, one might expect the information derived from elemental surface composition to be more accurate, yet care must be taken in interpreting such results. One should keep in mind that a given element when incorporated in glass versus crystalline mineral might behave differently. Farges et al. observed that crystalline quartz does not adsorb any sulfur species while amorphous silica does (Farges et al., 2009). The heterogeneous nature of the sample might further complicate finding the trends as elements forming different mineral phases will behave differently depending on the nature of mineral phase. For example, Fe is incorporated in both ilmenite (FeTiO_3) and fayalite (Fe_2SiO_4), yet the SO_2 uptake is significantly higher for the former mineral (Harris et al., 2012).

Earlier studies can be used to understand potential contribution of crystalline fraction of the volcanic ash to the uptake of SO_2 . Both quartz (SiO_2) and magnetite (Fe_3O_4) can be found in volcanic ash. Comparison of the uptakes of SO_2 on individual mineral oxides, such as CaO , Al_2O_3 , CaCO_3 , Fe_3O_4 and Fe_2O_3 showed that the uptake of SO_2 depends on the nature of the mineral oxide with higher uptakes observed when SO_2 interacted with iron-containing compounds (Usher et al., 2002). These observations were further tested by Zhang et al. who compared reactivity of different oxides taking into consideration their specific area and placed them in the following order: $\text{Fe}_2\text{O}_3 > \text{MgO} > \text{TiO}_2 > \text{FeOOH} > \text{mixture} > \text{Al}_2\text{O}_3 > \text{SiO}_2$ (Zhang et al., 2006). Both studies indicate that conversion of SO_2 per unit surface of Fe_2O_3 is the highest, suggesting that particles with the highest amount of iron might be the most reactive in reactions with SO_2 . Furthermore, the reactivity of the mixture, that was obtained by mixing the different oxides based on their abundance in the continental crust, was measured to be twice its theoretical value, which demonstrates its synergistic effect (Zhang et al., 2006). Even though most studies use simple mineral oxides and synthetic dust as a substitution for natural samples, such approach is problematic, as it undermines the importance of more complex mineralogy in the uptake of SO_2 . While studying the uptake of SO_2 on Saharan dust Harris et al. distinguished ilmenite (FeTiO_3), rutile (TiO_2) and iron oxides (Fe_2O_3 , Fe_3O_4 , FeOOH) ($\gamma_{\text{BET}}(\text{mixture of ilmenite and rutile}) = 3 \times 10^{-5}$) as major phases of dust responsible for uptake and oxidation of SO_2 (Harris et al., 2012). Uptake on feldspar minerals such as KAlSi_3O_8 , $\text{NaAlSi}_3\text{O}_8$ or $\text{CaAl}_2\text{Si}_2\text{O}_8$ and quartz (SiO_2) was found to be slow ($\gamma_{\text{BET}}(\text{feldspar}) = 9 \times 10^{-7}$, $\gamma_{\text{BET}}(\text{quartz with basic components}) = 4 \times 10^{-8}$) (Harris et al., 2012). To identify the elements associated with adsorption of SO_2 by crystalline material Harris et al. analyzed individual Saharan dust grains that were relatively rich in S content after their exposure to SO_2 and studied their elemental profile using single-particle SEM-EDX analysis (Harris et al., 2012). Ti, Fe and Ca were identified as the most important reactive elements, while Na, Mg, Al, Si showed no relationship to oxidizing capacity of dust (Harris et al., 2012). While studying the uptake of SO_2 on v-dusts it would be informative to investigate the uptake of SO_2 on other complex mineral phases present in v-dust such as pyroxene, plagioclase, amphibole, biotite, and olivine even though higher uptakes of SO_2 are linked to the presence of minerals lacking silicates, such as ilmenite (FeTiO_3) and magnetite (Fe_3O_4) (Harris et al., 2012).

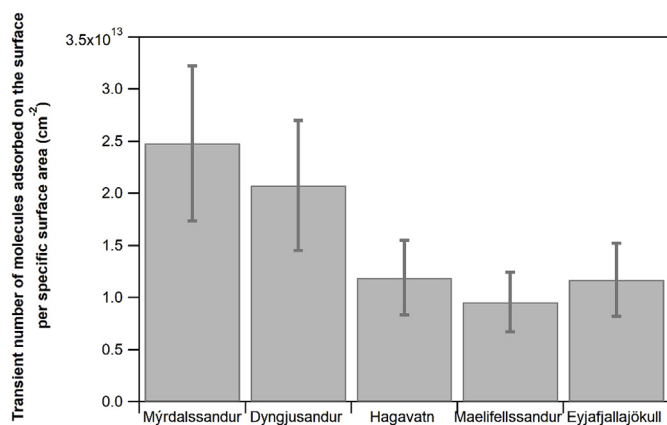


Fig. 7. Number of SO₂ molecules taken up on the surface of different v-dusts during the transient initial uptake process when exposed to [SO₂]₀ ≈ 75 ppb, T = 296K, RH = 30%, dark conditions. The errors quoted reflect the total error for the N_s determinations.

The number of SO₂ (N_s) molecules removed during the transient initial uptake process per surface area was also investigated and was calculated to be in the order of 10¹³ molecules cm⁻² (Table 3). These values are comparable to the values obtained by Maters et al., who reported the total uptake capacity of SO₂ on volcanic ash and glass powders under dry conditions at 10¹¹ to 10¹³ range (Maters et al., 2017). As with initial uptakes, total uptake capacity of SO₂ on the surface of synthetic volcanic glasses increased with decrease of their Si content and increase of their total Na, K, Mg, Ca content (Maters et al., 2017). As for the natural volcanic ash samples the relationship was less clear and the dependence on total surface Na, K, Mg, Ca content was suggested (Maters et al., 2017). Furthermore, as displayed in Fig. 7, the transient number of molecules adsorbed N_s at the initial stage of the exposure, and the steady state uptake coefficients do not follow the same trend. On one hand, Mýrdalssandur seems to adsorb the highest amount of molecules and it has the highest uptake coefficient. On the other hand, Hagavatn that has the smallest uptake coefficient adsorbs almost the same amount of molecules as Eyjafjallajökull and more than Maelifellssandur even though the latter two have an uptake coefficient that is twice as high as uptake coefficient of Hagavatn. The discrepancies between N_s and γ_{ss,BET} suggest that the surface is modified upon its initial exposure to SO₂. Indeed, one should keep in mind that

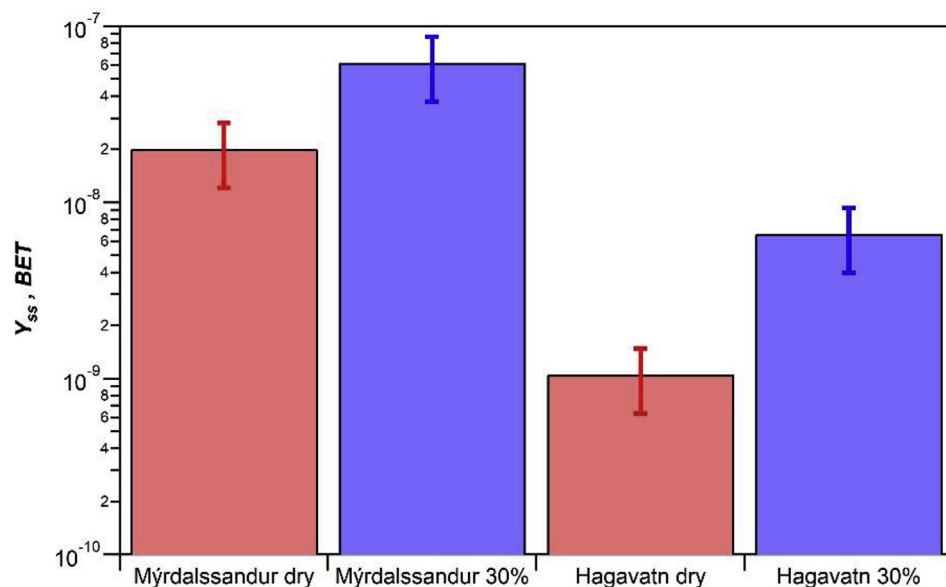


Fig. 8. Steady-state uptake coefficients of the Mýrdalssandur and Hagavatn v-dust samples at RH = 30% (blue bars) and RH = 0% (red bars), [SO₂]₀ ≈ 75 ppb, T = 296 K, under dark conditions. The errors quoted reflects the total error for the steady state uptake coefficient determination. (For interpretation of the references to color in this figure legend, the reader is referred to the Web version of this article.)

adsorption behavior of SO₂ on each volcanic dust was characterized by measuring the steady state uptake coefficients after 12 h of exposure, i.e. after long processing, while the number of molecules taken up was measured after the first 5 h of the interaction where a transient uptake was observed at the initial stage of the experiment. Differences in the observed trends could indicate that at the initial stage of the experiment the surface of the dusts is modified due to SO₂ uptake and the corresponding formation of sulfites and sulfates, and these modifications affect the surface reactivity at longer time scale when the γ_{ss,BET} values are determined. The modifications could explain why no correlation was noticed between the γ_{ss,BET} and N_s with the elemental composition of the v-dusts. Finally, the discrepancies could be due to the fact that the nature of the governing processes behind the initial fast uptake and thus the high amount of molecules adsorbed in the initial stage and those dominating the steady state uptake are fundamentally different (Huthwelker et al., 2006).

3.1.2. The role of relative humidity on the uptake of SO₂ on v-dusts

Several studies have highlighted the role of RH on SO₂ uptake (Li et al., 2006), (Zhou et al., 2014), (Huang et al., 2015). In order to investigate the role that RH plays in the steady state uptake of SO₂ on v-dust samples the relationship was investigated for two contrasted samples based on their steady-state uptakes – Mýrdalssandur and Hagavatn (Fig. 8). For Mýrdalssandur we observed that the steady state uptake coefficient of SO₂ at 30% of RH was significantly higher than under dry conditions (i.e. γ_{ss, BET} (30% RH) = 6.2 × 10⁻⁸ and γ_{ss, BET} (dry) = 2.0 × 10⁻⁸). For the Hagavatn v-dust a similar trend was observed (i.e. γ_{ss, BET} (30% RH) = 6.6 × 10⁻⁹ and γ_{ss, BET} (dry) = 1.0 × 10⁻⁹). The enhanced uptake trends observed in the presence of water indicate that water plays an important role promoting the partitioning of SO₂ to the adsorbed phase. There might be numerous reasons for the observed increased uptake of SO₂ in the presence of water vapor. Adsorbed water molecules can (i) participate in the reactions as reactants, (ii) serve as a medium for the reaction to take place or (iii) change the physical properties of the particle shifting the equilibrium towards higher SO₂ uptake. Water molecules can also form water layers that can help the product of the reaction to diffuse along the surface and thus promote the renewal, i.e. the turnover, of surface sites (Shang et al., 2010). The intrinsic ability of metal oxides to adsorb water molecules and form surface hydroxyls was linked to higher reactivity in the heterogeneous reaction with SO₂ (Zhang et al., 2006).

In the literature the analysis of the influence of RH on the uptake of

SO₂ on natural mineral dusts shows complex trends. An influence of water vapor on the interaction of SO₂ with Saharrah dust at 258 K showed no effect on initial uptake within statistical error (i.e. γ_{BET} (27% RH) = $(6.0 \pm 1.0) \times 10^{-5}$ and γ_{BET} (dry) = $(6.4 \pm 0.7) \times 10^{-5}$). Likewise, no dependency of the initial uptake coefficient on humidity was found for Adobe clay soil taken from Los Angeles area (Judeikis and Stewart, 1976). Alternatively, when Huang et al. subjected three authentic dusts to SO₂ at RH ranging from 0 to 90% an increase in uptake coefficient was observed for Tengger Desert dust (i.e. γ_{BET} (dry) $\approx 3.8 \times 10^{-5}$ and γ_{BET} (90% RH) $\approx 5.5 \times 10^{-5}$) and for Arizona test dust (i.e. γ_{BET} (dry) $\approx 1.3 \times 10^{-5}$ and γ_{BET} (90% RH) $\approx 2.76 \times 10^{-5}$), but a decrease was observed for Asian mineral dust (i.e. γ_{BET} (dry) $\approx 3.2 \times 10^{-5}$ and γ_{BET} (90% RH) $\approx 1.9 \times 10^{-5}$) (Huang et al., 2015). The negative dependence of humidity on SO₂ uptake in the case of Asian mineral dust was explained by the presence of water-soluble inorganic coating, which made surface more acidic and inhibited uptake of SO₂ (Huang et al., 2015). When the Asian mineral dust was washed and coating was removed, the uptake trend got reversed and showed positive correlation (i.e. γ_{BET} (dry) $\approx 0.85 \times 10^{-5}$ and γ_{BET} (90% RH) $\approx 1.32 \times 10^{-5}$) (Huang et al., 2015). Then again, while the samples from Inner Mongolian desert, characterized by high carbonate contents, demonstrated considerably increased uptakes at higher humidity (i.e. $\gamma_{\text{ss, BET}}$ (40% RH) = 1.0×10^{-6} and $\gamma_{\text{ss, BET}}$ (dry) = 1.7×10^{-7}), Xinjiang sierozem natural mineral dust showed only a modest increase in steady-state uptake (i.e. $\gamma_{\text{ss, BET}}$ (40% RH) $\approx 2.4 \times 10^{-7}$ and $\gamma_{\text{ss, BET}}$ (dry) $\approx 2.2 \times 10^{-7}$) (Adams et al., 2005). The authors suggest that difference in the mineralogy could be responsible for the difference in the observed trends (Zhou et al., 2014). Higher carbonate component of the Inner Mongolian desert dust can promote the SO₂ uptake. Indeed, while investigating carbonate particles Zhang et al. observed that the value of the steady state uptake $\gamma_{\text{ss, BET}}$ drastically increases from $\gamma_{\text{ss, BET}}$ (1%) = 0.32×10^{-8} to $\gamma_{\text{ss, BET}}$ (85% RH) = 13.9×10^{-8} , at 85% RH reaching 43 times its value at 1% (Zhang et al., 2018). In our study volcanic dusts, void of carbonates, cannot be directly compared to carbonate-rich samples, but the observed trend follows the one of Tengger Desert dust and Arizona test dust discussed earlier. More information about influence of humidity on the steady state uptake of SO₂ on the surface of volcanic glass and ash is necessary to obtain a more comprehensive picture.

While the increase in the SO₂ uptake with the increase of relative humidity is observed for a number of samples, it is not at all the case for the uptakes of other species, such as nonpolar volatile organic compounds (Romanias et al., 2016), hydrogen peroxide (H₂O₂) (Romanias et al., 2012) or ozone (O₃) (Lasne et al., 2018). In fact, the uptake coefficient can decrease with increased humidity, such as the case for the steady state uptake of O₃ on montmorillonite clay dust reflecting the tendency for the molecules in question and molecules of water to compete with each other for the sorptive sites on the clay surface (Lasne et al., 2018).

The observation of the steady state nature of the uptakes points out that there are important and maybe cyclic processes occurring on the surface of the v-dust. The gas phase monitoring limits us to the determination of kinetic parameters; in order to investigate the mechanism of the SO₂ uptake surface monitoring is necessary. Increased SO₂ uptake at higher RH suggests that humidity plays a particularly important role in the adsorption of SO₂ to the surface. To monitor the adsorbed phase, determine the functional groups that are involved in the adsorption of SO₂ and to further evaluate the role of water to the reaction system, a series of experiments were carried out employing DRIFT spectroscopy.

3.2. Exploring SO₂ uptake on v-dust from the adsorbed phase: DRIFTS study

While flow tube reactor monitors changes in the gas-phase concentration, DRIFTS focuses on changes on the solid phase. It is

commonly used to study fine particles and powders, and can be used to investigate adsorption of molecules on solid surfaces. In this case spectra are collected as difference spectra with the unexposed solid as background. As the reaction proceeds, growing or decreasing peaks can be attributed to the species formed or consumed on the surface. Infrared spectroscopy based on light diffuse reflectance offers information about the vibrational modes associated with stretching, bending, and rocking motions of the adsorbed molecules. However, in order to monitor these vibrations the sample has to have high enough reflectance to insure an adequate signal in response to changes in the adsorbed phase, and the surface concentration needs to be high enough due to the low sensitivity of the technique. If the sample is highly absorbent, which is the case of v-dust samples, it is usually diluted in a non-absorbent matrix, such as KBr. In our case, however, this type of matrix could not be used because of the interactions of KBr with SO₂ and thus the use of pure v-dust was required. The background obtained for each v-dust under dry conditions showed that all of them absorb light strongly and, as a result, a weak IR signal was recorded in response to changes in the adsorbed phase. To study the adsorption of SO₂ on v-dust, backgrounds of five samples were taken to choose the least absorbent varieties. In comparison with other v-dusts the background for Hagavatn and Eyjafjallajökull shows higher reflectance in the area from 800 to 1350 cm⁻¹ where sulfite and sulfate species usually absorb. Because of its higher reflectance and higher specific surface area, Hagavatn v-dust was selected as the most appropriate sample for DRIFTS experiments. Besides, results obtained from the flow tube studies showed similar trends in SO₂ adsorption by the v-dusts based on gas-phase monitoring of SO₂, i.e. rapid consumption of SO₂ gas at the initial stage of surface exposure followed by a steady state removal of the probe molecule. Therefore, it appeared justified to choose one dust as a representative sample to study the mechanism of product formation on the surface of aerosols. Aiming to further investigate the observations from the flow tube study and to further assess the role of humidity on the reaction mechanism, the DRIFTS experiments were performed under dry conditions and 30% RH using Hagavatn as a sample material.

3.2.1. Typical DRIFT spectra of SO₂ interaction on v-dust

Fig. 9 and Fig. 10 show DRIFT spectra of Hagavatn v-dust at increasing SO₂ exposure time intervals at room temperature under 0% and 30% RH respectively. Table 4 introduces the assignment of peaks of different adsorbed sulfur-containing species as well as water and hydroxyl groups on the surface of v-dust investigated and different metal oxides found in the literature.

In Particular, the negative and positive absorption peaks in the area from 4000 to 3500 cm⁻¹ correspond to the free OH groups that are naturally present on the surface of v-dust (Hair, 1975). These groups are attached to the surface atoms, such as Si for example, and can be either completely isolated or hydrogen-bonded to each other (Hair, 1975). Adsorption of molecules containing a lone-pair of electrons is often associated with isolated surface OH groups, while neighboring hydrogen-bonded surface OH groups are involved in the adsorption of water (Hair, 1975), (Nanayakkara et al., 2012). The exact assignment of each individual peak is not possible due to the complex response reflecting slightly different vibrational energies of OH groups bonded to different minerals composing the v-dust. A peak from 3500 to 2600 cm⁻¹ and another peak from 1800 to 1400 cm⁻¹ centered at 1620 cm⁻¹ (not displayed) are attributed to vibration modes in molecular water (Hair, 1975).

A weak broad peak from 2600 to 2400 cm⁻¹, visible under humid conditions, could be assigned to the S–H stretch vibration of the HSO₃⁻ bisulfite species that is only found in the literature as a theoretical value calculated by Zhang et al. for aqueous solution and reported to be in the range of 2620 to 2450 cm⁻¹ (Zhang and Ewing, 2002). This peak is not visible under dry condition. Sulfur-containing products appear in the area from 1385 to 700 cm⁻¹ under humid conditions and from 1367 to 716 cm⁻¹ under dry conditions. Spectra under humid conditions are

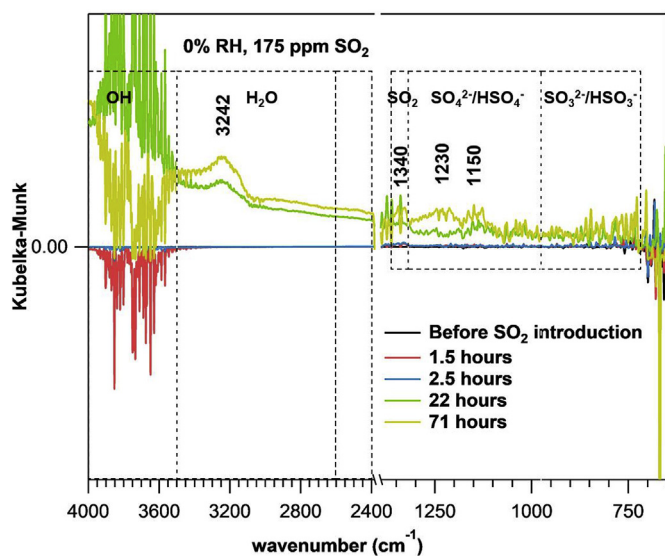


Fig. 9. DRIFTS spectra of SO_2 uptake by Hagavatt v-dust at 0% RH and 296 K depicting evolution of bands for free surface OH groups ($4000\text{--}3500\text{ cm}^{-1}$), adsorbed water ($3500\text{--}2600\text{ cm}^{-1}$), physisorbed SO_2 ($1385\text{--}1320\text{ cm}^{-1}$), sulfates/bisulfates ($1320\text{--}975\text{ cm}^{-1}$), sulfites/bisulfites ($975\text{--}716\text{ cm}^{-1}$) as a function of time: black line – before introduction of SO_2 , red line–after 1.5 h of exposure to SO_2 , blue line–after 2.5 h of exposure to SO_2 , green line–after 22 h of exposure to SO_2 , yellow line–after 71 h of exposure to SO_2 . (For interpretation of the references to color in this figure legend, the reader is referred to the Web version of this article.)

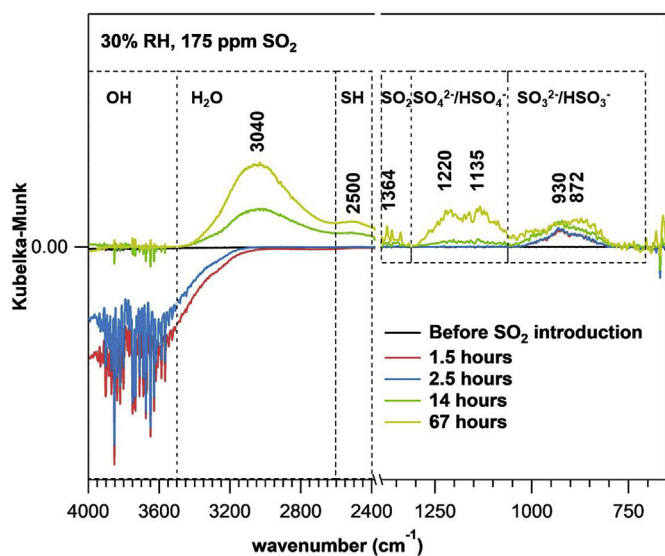


Fig. 10. DRIFTS spectra of SO_2 uptake on Hagavatt v-dust at 30% RH and 296 K depicting evolution of bands for free surface OH groups ($4000\text{--}3500\text{ cm}^{-1}$), adsorbed water ($3500\text{--}2600\text{ cm}^{-1}$), SH groups ($2600\text{--}2400\text{ cm}^{-1}$), physisorbed SO_2 ($1367\text{--}1320$), sulfates/bisulfates ($1302\text{--}1050\text{ cm}^{-1}$), sulfites/bisulfites ($1053\text{--}700\text{ cm}^{-1}$) as a function of time: black line – before introduction of SO_2 , red line–after 1.5 h of exposure to SO_2 , blue line–after 2.5 h of exposure to SO_2 , green line–after 22 h of exposure to SO_2 , yellow line–after 71 h of exposure to SO_2 . (For interpretation of the references to color in this figure legend, the reader is referred to the Web version of this article.)

better resolved and several peaks can be distinguished: 3040 , 2500 , 1364 , 1220 , 1135 , 930 and 872 cm^{-1} . Peaks under dry conditions are much noisier, nevertheless the following peaks are observed: 3242 , 1340 , 1230 and 1150 cm^{-1} . A double peak centered at 1364 cm^{-1} under humid conditions and at 1340 cm^{-1} under dry conditions appears rapidly upon exposure of the surface to SO_2 gas and disappears

right away from the spectra after ceasing the SO_2 flow. It was therefore assigned to the weakly, reversibly physisorbed SO_2 species. The peak corresponds well to the literature values for SO_2 adsorption under dry conditions on the surfaces of aluminum, magnesium or titanium oxides identified in the previous studies at 1330 cm^{-1} and its gas-phase value of 1362 cm^{-1} (Nanayakkara et al., 2012), (Goodman et al., 2001). Another band appears rapidly upon exposure of SO_2 to the surface between 1053 and 700 cm^{-1} under humid conditions. A corresponding band between 975 and 716 cm^{-1} under dry conditions takes more time to develop and is hard to interpret since its intensity is almost at the limit of detection of the DRIFTS instrument. The assignment of this band is based on the previous assignments of SO_2 adsorption on the surface of different metal oxides found in the literature and corresponds to the stretching motion of sulfite and bisulfite species that are bonded to the surface in a monodentate or bidentate mode. Different coordination environments as well as heterogeneous nature of v-dust contribute to the broadening of the band (Usher et al., 2002). In particular, Goodman et al. (2001), Usher et al. (2002) and Zhang et al. (2006) assigned the band between 1100 and 850 cm^{-1} to adsorbed sulfite and bisulfite on $\alpha\text{-Al}_2\text{O}_3$ and MgO. Li et al. (2006) and Wu et al. (2011) assigned a $1000\text{--}900\text{ cm}^{-1}$ band on CaCO_3 to a stretching vibration of sulfite. A peak from 1200 to 800 cm^{-1} on TiO_2 was assigned to sulfite and bisulfite species by Nanayakkara et al. (2012). On hematite particles Wang et al. assigned to sulfites a peak between 950 and 800 cm^{-1} under dry conditions and a series of peaks from 1050 to 900 cm^{-1} under humid conditions (Wang et al., 2018b). Finally, a band from 1320 to 975 cm^{-1} with features at 1230 and 1150 cm^{-1} in dry conditions and from 1302 to 1055 cm^{-1} with features at 1220 and 1135 cm^{-1} under humid conditions was attributed to sulfate and bisulfate species. The assignment agrees well with the results published previously, where sulfates/bisulfates were found around $1300\text{--}1100\text{ cm}^{-1}$ on $\alpha\text{-Al}_2\text{O}_3$ and MgO (Usher et al., 2002), (Zhang et al., 2006); between 1240 and 1012 cm^{-1} on CaCO_3 with features at 1198 , 1127 , and 1090 cm^{-1} (Wu et al., 2011), (Li et al., 2006). Sulfates were reported between 1300 and 1100 cm^{-1} on TiO_2 (Nanayakkara et al., 2012), (Shang et al., 2010); and at 1220 cm^{-1} on Fe_2O_3 (Wang et al., 2018b). Just as sulfites, sulfates can be bonded to the surface in bidentate or monodentate modes (Jiang et al., 2010). A peak centered at 1220 cm^{-1} under humid conditions and at 1230 cm^{-1} under dry conditions could be attributed to the formation of bisulfate species (Wang et al., 2018a). The process of sulfate/sulfite formation is explained later in the reaction mechanism section.

3.2.2. Surface reaction mechanism

Changes in the DRIFT spectra of the surface of Hagavatt v-dust are clearly seen upon introduction of SO_2 (Figs. 9 and 10). In comparison with the studies of the interaction of SO_2 with pure metal oxides reported earlier by different researchers, it is evident that the peaks for sulfur-containing species appear much slower, most probably due to low sensitivity when dealing with dark v-dusts where the reflectance of the infrared light is limited (Zhang et al., 2006), (Usher et al., 2002), (Goodman et al., 2001), (Li et al., 2006), (Wu et al., 2011), (Nanayakkara et al., 2012), (Shang et al., 2010), (Wang et al., 2018b). The time evolution of five peaks corresponding to different species, such as free OH groups, molecular water, physisorbed SO_2 , sulfites/bisulfites and sulfates/bisulfates is followed.

3.2.2.1. Dry conditions. From our flow tube experiments presented earlier it is apparent that SO_2 gas is massively lost from the gas phase upon its exposure to the v-dust surface. Interestingly, the first peaks that appear in the DRIFT spectra after introduction of SO_2 gas are positive peaks for physisorbed SO_2 gas and negative peaks for free OH groups (Fig. 9). Note that although the sample has been thermally pretreated and the experiment is performed under dry conditions, surface OH groups are present on the surface of the sample. The complete dehydroxylation of the surface would have required stronger thermal

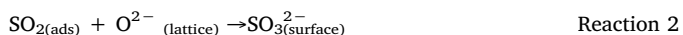
Table 4
Vibrational wavenumbers (cm^{-1}) of sulfur-containing species adsorbed on v-dust and metal oxides.

Molecular species (wavenumbers are expressed in cm^{-1})	V-dust (this work)	Si_2O_3	Al_2O_3	MgO	TiO_2	CaCO_3	Fe_2O_3	Theoretical calculations
SH stretch of HSO_3^-	2600–2400	2600-2400 (Hair, 1975)						
SO_2	1364, 1340	1330, 1149 (Goodman et al., 2001)	1330, 1149 (Goodman et al., 2001)	1330, 1149 (Goodman et al., 2001)	1139, 1325 (Nanayakkara et al., 2012)		1400 (Nanayakkara et al., 2012)	2620 to 2450 (Zhang and Ewing, 2002)
$\text{HSO}_3^-/\text{SO}_3^{2-}$	1053–700 975–716	1200-900 (Goodman et al., 2001)	1200-900 (Goodman et al., 2001)	1100-850 (Zhang et al., 2006)	1200-800 (Nanayakkara et al., 2012) 1080 (Shang et al., 2010)		Dry: 950–800 Humid: 1050-900 (Wang et al., 2018b)	
SO_3^{2-}				1125-800 (Goodman et al., 2001)	Monodentate: 1033, 971, 923 (Nanayakkara et al., 2012) Bidentate: 1006, 886(Nanayakkara et al., 2012) 1077 (Nanayakkara et al., 2012)	1000-900 (Li et al., 2006) 1000-885 (Wu et al., 2011)	Dry:891 (Wang et al., 2018b) Humid: 981 (Wang et al., 2018b)	
HSO_3^-								
$\text{HSO}_4^-/\text{SO}_4^{2-}$	1320–975 1302–1055 1220, 1230	1245, 1170 (Usher et al., 2002)		1150, 1050 (Usher et al., 2002)		1240-1012 (Wu et al., 2011)		1054, 1154, 1219 (Zhang and Ewing, 2002)
HSO_4^-							1219 (Wang et al., 2018a)	
SO_4^{2-}							Dry: 1339–1014 Humid: 1208-1222(Wang et al., 2018b)	
free OH groups	4000–3500	1300-1100(Zhang et al., 2006)	3748, 3707 (Goodman et al., 2001)	1300-1100 (Zhang et al., 2006)	1361, 1297, 1172, 1116, 1050, 1000 (Nanayakkara et al., 2012) 1300-1100 (Shang et al., 2010)	1130 (Li et al., 2006)		
OH groups of acids								
molecular water	3500–2600 1400–1800	3450, 1630 (Hair, 1975)	4000-3500 (Hair, 1975)	3800-3600 (Nanayakkara et al., 2012) 1666, 3628 (Shang et al., 2010)	3800-3600 (Nanayakkara et al., 2012) 1666, 3628 (Shang et al., 2010)		1208-1222(Wang et al., 2018b) 3704 (Wang et al., 2018b) 3447, 3548 (Wang et al., 2018b) 3208, 1642 (Wang et al., 2018b)	3622 (Zhang and Ewing, 2002)

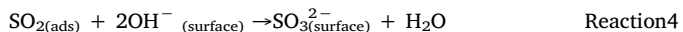
pretreatment. The loss of surface free OH groups reaches its local minimum at around 1.5 h exposure to SO₂ before returning to its initial pre-exposed level where it starts fluctuating around zero. The peak for SO₂ gas is stable, but hard to integrate due to its small size and overlap with a much more pronounced peak for bulk water. Bulk water peak is highly unstable. The disappearance of free OH groups and appearance of physisorbed SO₂ suggest that in the first instants of the reaction, SO₂ gas gets weakly bonded to hydroxyl groups of the surface as first proposed by Datta et al. and later proved by theoretical calculations by Lo et al. for γ -alumina (Datta et al., 1985), (Lo et al., 2010). Maters et al. suggested that due to the weakly acidic nature of SO₂ gas its uptake is likely to happen on strongly basic sites affiliated with alkaline and alkaline earth metals on the surface of the volcanic glass (-K-OH, -Mg-OH, -Ca-OH, Mg-OH) (Maters et al., 2017). At the same time it is also possible for the SO₂ gas to get adsorbed on metallic Lewis acid sites of mineral phase as proposed by Wang et al. (2018a). Hence, the first interaction of SO₂ gas with the surface under dry conditions is its distribution on different sites of the v-dust leading to a reversible physisorption of SO₂, as indicated by subscript (*ads*) (Reaction 1). Throughout the manuscript the chemisorbed species or chemical groups that form a chemical bond with the surface are indicated as (*surface*).



Physisorbed SO₂ can then participate in reactions leading to chemisorbed species. Sulfites and sulfates, under dry conditions first appear after several hours of exposure probably due to the low sensitivity of our DRIFT setup, as abovementioned. Sulfites can be formed on the lattice oxygen sites that can be viewed as Lewis basic sites (Wang et al., 2018a) as in Reaction 2.

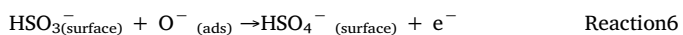
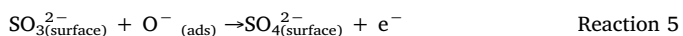


Alternatively, sulfites can be formed in the presence of hydroxyl groups as SO₂ can react with either one hydroxyl group to form bisulfite (Reaction 3) or two neighboring hydroxyl groups to form sulfite and water (Reaction 4) (Wang et al., 2018a). Surface hydroxyl groups themselves can be bonded to a single metal atom or bridge two, creating different environments for interactions with SO₂ (Ullerstam et al., 2002).



Chemisorption of SO₂ gas on oxide anions (O²⁻) and hydroxyl groups of volcanic ash and glass leading to the formation of sulfites and bisulfites was suggested earlier by Maters et al. and detection of sulfites in the leachates confirmed the conversion (Maters et al., 2017).

From Fig. 11 that shows time evolutions of sulfites and sulfates, it can be observed that, under dry conditions, sulfites (SO₃²⁻) get completely stabilized after 22 h of exposure, but sulfates (SO₄²⁻) keep growing linearly, suggesting that sulfites are the intermediate species in the oxidation of SO₂ to sulfates. Oxidation of sulfites to sulfates on the surface of volcanic glass was observed by Farges et al. (2009). Sulfites can be oxidized to sulfates via several pathways. Active oxygen derived from molecular oxygen adsorbed on the active sites (Reaction 7) can oxidize sulfites to sulfates and bisulfites to bisulfates as in Reaction 5 and Reaction 6 (Wang et al., 2018a).



Contrary to our observations and to results reported by Shang et al. (2010), who also noticed a stable rate of sulfate production on the surface of titanium dioxide particles in the presence of oxygen, Usher et al. (2002) noted complete saturation of mineral oxide surfaces with SO₂ gas and observed no sulfate formation even upon exposure of SO₂-treated surface to air and oxygen. It could be due to the fact that the

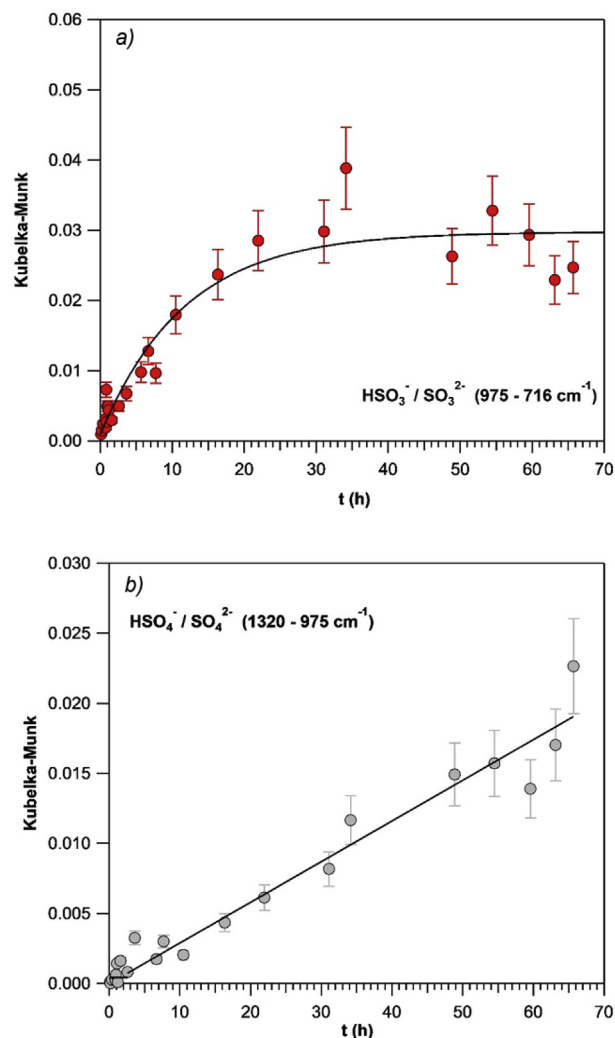
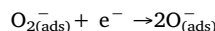


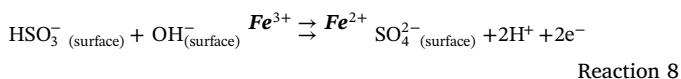
Fig. 11. Integrated absorbance for (a) sulfites/bisulfites, (b) sulfates/bisulfates as a function of time under 0% RH and 296K. Upper graph: sulfites/bisulfites are stabilized after 22 h of exposure. The solid line is an exponential fitting of experimental results to better display the observed trends. Lower graph: A linear growth of sulfates/bisulfates with time is noticed; note that the peak is stable for the first couple of hours and then keeps increasing in a linear fashion. The solid line is the linear fit of experimental results.

minerals under investigation were not able to convert molecular oxygen into active oxygen under the specific experimental conditions of these measurements.

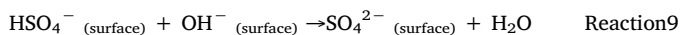


where e^- is a conductive electron trapped in the vacant oxygen site on the surface of some oxides that are prone to having defect sites, such as on the surface of Fe₂O₃, for example (Wang et al., 2018b), (Baltrusaitis et al., 2007). Noticeably, reaction proceeds in the absence of light (Baltrusaitis et al., 2007). Reaction 7 was reported to enable the conversion of sulfites to sulfates on the surface of mineral phase, but a similar process can be expected to happen on the amorphous fraction of the volcanic ash due to the high defect population on silicate glasses (A Leed and Pantano, 2003), (Farges et al., 2009).

Additionally, certain metal centers that can be readily reduced, such as Fe³⁺ to Fe²⁺, contribute to the formation of sulfates from bisulfites as per Reaction 8 (Wang et al., 2018a).



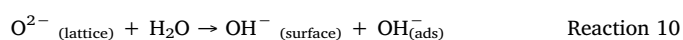
Finally, bisulfates can be oxidized to sulfates by hydroxyl groups as per [Reaction 9](#) ([Wang et al., 2018a](#)).



On ceasing the gas flow and flushing the system for 6 h, the peak for sulfites decreases due to its oxidation as per [Reaction 5](#), [Reaction 6](#) and [Reaction 8](#), while the peak for sulfates increases for a couple of hours before getting stable, at the same time slightly changing its shape. The peak centered at 1230 cm^{-1} gets smaller in comparison with the peak at 1135 cm^{-1} suggesting indeed further conversion of bisulfates to sulfates. A decrease in sulfite peak with simultaneous increase in the sulfate peak upon cutting off SO_2 supply and addition of O_3 was observed by [Li et al. \(2006\)](#). Thus, sulfates appear to be the final product of oxidation of SO_2 gas and they keep being formed on the surface as long as there are sulfites available for oxidation. Sulfates were also reported as a final irreversible product of the interaction of SO_2 gas with volcanic glass by [Farges et al.](#) and by [Maters et al. \(Farges et al., 2009\)](#), ([Maters et al., 2017](#)).

3.2.2.2. Humid conditions. After exposure of v-dust to SO_2 gas under humid conditions the following changes are observed in the analysis of

DRIFT spectra as seen in [Figs. 10](#) and [12](#). At the very beginning of the experiment, the free OH groups get consumed and reach a minimum after 1.5 h exposure to SO_2 , at the same time sulfites form rapidly and at an almost linear rate. The peak for physisorbed SO_2 increases much slower and the peak remains small for the duration of the experiment. The initial time period corresponds well with the reaction mechanism proposed by [Wang et al.](#) in [Reaction 3](#) and [Reaction 4](#) both of which require consumption of free OH groups to produce sulfites and bisulfites. From 1.5 to 2.5 h consumption of OH groups slows down and finally reaches a stable level. It is important to stress out that, when working under humid conditions, surface OH groups are continuously regenerated. The mechanism for metal oxide surface hydroxylation proposed by [Tamura et al.](#) assumes that an exposed oxygen center of the metal oxide lattice acts as Lewis base with water to form a surface terminal hydroxyl group and a hydroxide ion as shown in [Reaction 10](#) ([Tamura et al., 2001](#)). In other words, a surface oxide ion gets neutralized by water to become $\text{OH}^- (\text{surface})$, while water itself loses a proton to become hydroxide ion $\text{OH}^- (\text{ads})$.



Sulfates are first observed in the DRIFT spectra at 2.5 h exposure to SO_2 . Sulfates can be formed by three different pathways shown in [Reaction 5](#), [Reaction 6](#), and [Reaction 8](#) ([Wang et al., 2018a](#)). Unlike sulfites, the peak for sulfates keeps growing linearly with time once

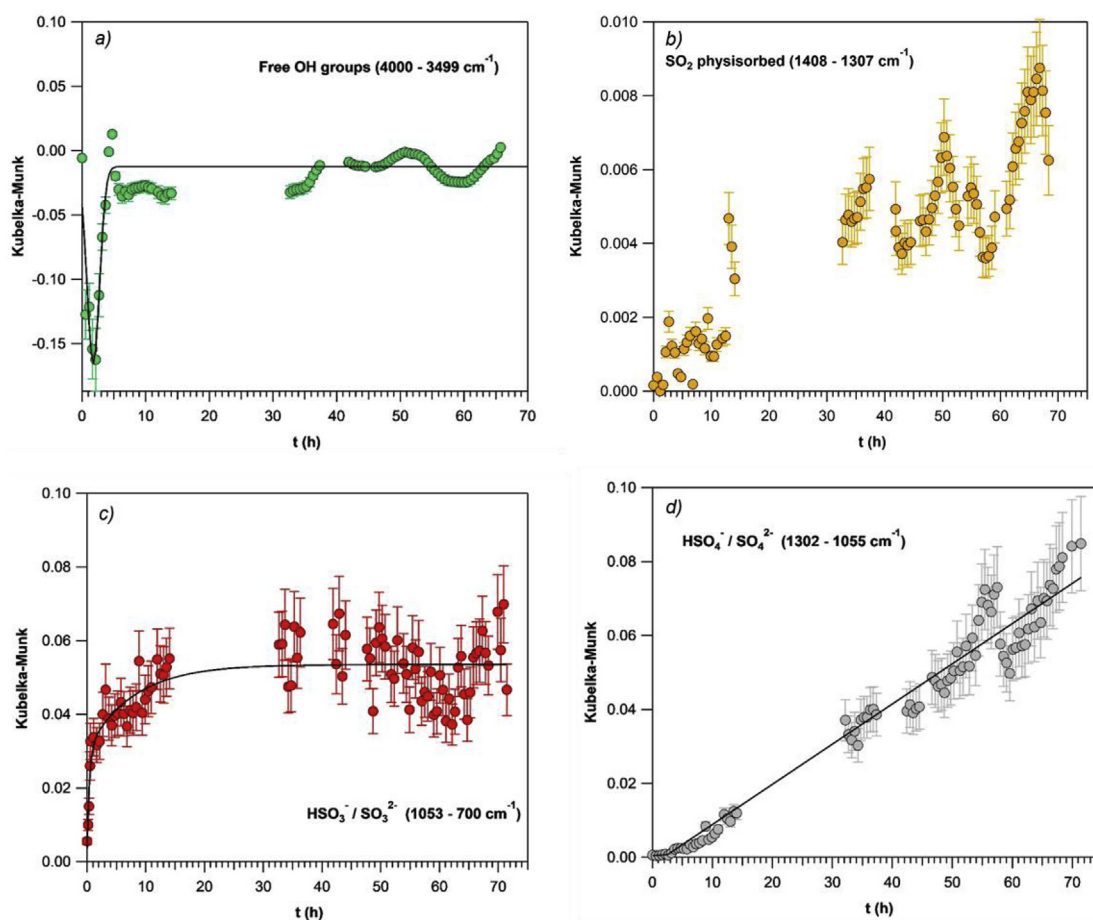


Fig. 12. Integrated absorbance for (a) free hydroxyl groups, (b) physisorbed SO_2 , (c) sulfites/bisulfites, (d) sulfates/bisulfates as a function of time under 30% RH and 296 K. The free OH groups get consumed very fast at the beginning of the experiment and reach a minimum at 1.5 h, then the consumption of OH groups decreases and reaches a stable level at 2.5 h. The solid line is an empirical fitting of experimental results to better display the observed trends. The peak for physisorbed SO_2 is quite noisy but increases slowly and remains weak for the duration of the experiment. The solid line is an empirical fitting of experimental data points. Sulfites/bisulfites grow rapidly and almost linearly for the first 1.5 h and then stabilize. The solid line is an exponential fitting of experimental results to better display the observed trends. The peak for sulfates/bisulfates is stable at low values for the first 2.5 h and then increases in the linear fashion. The solid line is the linear fit of experimental results.

again suggesting that sulfate is the final product of SO₂ oxidation and that the surface does not get saturated within the duration of the experiment. A peak for molecular water is hard to evaluate at 30% RH as water is being constantly supplied in large excess. Initially, the peak for water seems to decrease, which could be due to the competition with SO₂ gas molecules for active sites on the surface (Fig. 10). At 14 h the water peak stabilizes at a positive value, indicating that the surface is now storing more H₂O molecules than before introduction of SO₂ gas (Fig. 10). Formation of sulfite and sulfate species could have changed equilibrium for adsorption of water on the dust surface (e.g. due to chemical changes of the mineral structure that increase the hygroscopicity of the samples). Particularly, it was argued that adsorption of bidentate sulfate on the surface of Fe–Mn/TiO₂ catalyst increases the Lewis acid character of the metal ion to which it is attached, thus potentially favoring the adsorption of water on the metal center (Jiang et al., 2010). Finally, when the flow of SO₂ is stopped, the peak for sulfite gradually decreases while the peak for sulfate increases for a couple of hours, stabilizes and stays in the spectra for at least 6 h. Like under dry conditions the peak for bisulfates/sulfates changes its shape by decreasing the peak associated with bisulfates (at 1220 cm⁻¹) suggesting its conversion to sulfates.

3.2.2.3. Comparison between dry and humid conditions. Although DRIFTS is a semi-quantitative technique, it is feasible to compare the results obtained under dry and humid conditions. Thus, in comparison with the reaction under dry conditions the reaction under humid conditions is much more pronounced, resulting in both faster reaction rates and higher integration values obtained for all sulfur containing species involved. This observation is in line with the results obtained from the flow tube experiments, where significantly higher steady state uptakes were determined for SO₂ under humid compared to dry conditions. Faster sulfite formation is most likely related to the dramatic increase in the amount of hydroxyl groups covering the surface under humid conditions, driving the sulfite and bisulfite formation through Reaction 3 and Reaction 4. Indeed, under humid conditions the amount of hydroxyl groups lost in the first minutes is much larger than under dry conditions, thus adsorbed SO₂ molecules convert rapidly to form sulfites (Figs. 9 and 10). Huang et al. reported that the rate of sulfate formation on the surface of Arizona test dust increased with RH and reached its maximum at 70% RH (Huang et al., 2015). Importance of surface OH groups in the heterogeneous oxidation of SO₂ gas was discussed by Zhang et al. who compared basic, neutral and acidic Al₂O₃ in their ability to oxidize SO₂ and noted that basic Al₂O₃ was much more efficient due to its higher concentration of hydroxyl groups on the surface (Zhang et al., 2006). It was also suggested that reactivity of different oxides to SO₂ uptake could be predicted by evaluating their intrinsic ability to form surface hydroxyl groups. Thus, metal oxides that have empty or half-empty d atomic orbitals, such as Al₂O₃, easily adsorb molecular oxygen and gaseous water and show excellent performance in the reactions with SO₂ while metal with full d orbitals, such as MnO₂, show weak reactivity (Zhang et al., 2006). Reaction of SO₂ gas with the lattice oxygen as in Reaction 2 seems to proceed much slower. The observation is in line with the results of experiments on dehydroxylated surfaces that show very little reactivity towards product formation, suggesting low reactivity of lattice oxygen groups (Nanayakkara et al., 2012). Absence of S–H stretch from the spectra of the v-dust under dry conditions could be due to the fact that bisulfites and bisulfates are formed in much lower quantities than in humid conditions.

3.2.2.4. Surface coverage of v-dust with SO₄²⁻ ions. The uptake of SO₂ gas on the surface of the v-dust proved to be very long and the process of conversion to H₂SO₄ was not declining for as long as the SO₂ gas was supplied, at least for the duration of the experiments. At the same time no product leaving the surface was identified. This is puzzling since there seems to be no reason for continuous uptake in the absence of

some kind of catalytic process leading to regeneration of active sites. In this case it only makes sense that sooner or later the process should come to an end. In order to evaluate a potential for further uptake and conversion of SO₂ to H₂SO₄ it was decided to evaluate the surface coverage of SO₄²⁻ at the end of the experiment. The amount of the product formed on the surface was quantified using HPLC. A 109 mg sample of Hagavatt dust was exposed to 175 ppm of SO₂ gas for 24 h at 23 °C and 30% RH and then flushed for 6 h to allow complete oxidation of sulfites into sulfates. The dust was then extracted in 1 mL of 1% formalin. A calibration curve was constructed using Na₂SO₄ as a standard solution. The amount of SO₄²⁻ recovered was calculated at 62.79 µg corresponding to 0.57 mg of SO₄²⁻ ion per 1g of Hagavatt dust. The number of molecules formed after 24 h of continuous exposure was calculated as 7.95 × 10¹³ molecules cm⁻². Considering the linear trend that we observed in DRIFTS experiments, the coverage of SO₄²⁻ ions after 72 h of exposure was estimated at ca. 2.3 × 10¹⁴ molecules cm⁻². To approximate whether the monolayer coverage was reached it was decided to compare the amount of molecules formed on the surface to its theoretical monolayer coverage.

The calculated value for the amount of sulfuric acid molecules necessary to form a monolayer was calculated to be 4.22 × 10¹⁴ molecule cm⁻². This value is consistent with the usually reported surface density of sorptive sites on mineral oxides, ca. 3 × 10¹³–5 × 10¹⁴ sites cm⁻² (Kulkarni and Wachs, 2002). The coverage of SO₄²⁻ ions after 72 h of exposure was estimated to be almost by a factor of 2 lower than the theoretical monolayer coverage of the sample by H₂SO₄ molecules. At this point it should be noted that experimentally, the molecules are not expected to pack together perfectly since the shape of the molecules and hindering interactions would render some of the active sites on the surface inaccessible. Thus, the experimental monolayer coverage would be assumed to be lower than the theoretical one (Hudson et al., 2002), (Diaz et al., 2005).

The rough approximation points to the fact that the surface coverage θ after 72 h of exposure is approximately $\theta = 0.5$. Therefore, it can be concluded that there are still available sites on the surface of v-dust for the conversion of SO₂ to occur and the subsequent sorption of sulfates. Moreover, the process does not seem to slow down. Longer exposure times are necessary to determine how the sulfate formation will behave at $\theta = 1$ when a monolayer of sulfate ions forms. Further on, what happens after the formation of monolayer? Will the process stop, and if it continues what are the driving forces behind it?

4. Conclusions and atmospheric implications

In this study the uptake of SO₂ gas by Icelandic v-dust was investigated. Uptake of SO₂ by v-dusts was observed even though all of them have already been exposed to SO₂ in the volcanic conduit and plume owing to their production/emission mode. Upon exposure of the v-dust to SO₂ the system reaches a steady state clearly distinct from the initial state indicating continuous consumption of SO₂ molecules. The steady state uptake coefficients for v-dusts at 30% RH range from (6.6 ± 2.6) × 10⁻⁹ for Hagavatt to (6.2 ± 2.5) × 10⁻⁸ for Mýrdalssandur. Moreover, increased uptake of the SO₂ gas in humid conditions suggests that water plays an important role in the above-mentioned processes. The DRIFTS data indicate the presence of sulfite and sulfate ions on the surface. Presence of sulfates was further detected by HPLC analysis and it was also noted that after 3 days of exposure of v-dust to 175 ppm SO₂ the surface coverage by SO₄²⁻ ions is ca. $\theta = 0.5$, i.e. lower than the monolayer coverage suggesting that the surface of the v-dust is still active in uptake processes that are occurring on the surface. It is most likely that SO₂ gas reacts at the surface of the v-dust and forms sulfites or bisulfites, which are then converted to sulfates. Hydroxyl groups play a major role in the conversion of SO₂ gas to sulfites, while oxidizing agents in the form of active oxygen or metal centers are necessary to their conversion to sulfates. Furthermore, sulfates formed on the surface of v-dust are a stable chemisorbed species

not easily desorbed even after flushing for hours in the absence of SO₂ gas.

During an episode of volcanic eruption volcanic dust will react with SO₂ gas both in subvolcanic and atmospheric environments (Renggli et al., 2019), (Schmauss and Keppler, 2014). Initially, at near-magmatic high temperatures of over 800 °C there is a compelling evidence that the adsorption of SO₂ gas is driven by diffusion of Ca²⁺ cations from the interior of the glass to its surface followed by precipitation of CaSO₄ (Delmelle et al., 2018). This initial stage is characterized by high concentration of gases and high density of ash particles, but is very short in duration lasting only a couple of minutes even in the case of Earth's largest explosive eruptions (Delmelle et al., 2018). The pathway is of limited importance in small and medium size eruptions and/or eruptions of volcanoes lacking a deep-seated magma chamber (Ayris et al., 2013). Subsequent cooling rapidly brings the system to the subzero temperatures (Textor et al., n.d.). At ambient and low temperatures where effective diffusion of cations to the ash surface is no longer possible the driving force of SO₂ adsorption is its physisorption on the surface of ash followed by chemical reaction with active sites that are available on the surface. Previous research under these conditions points out that the rate of sulfate formation is higher at low temperatures compared to room or elevated temperatures of up to 150 °C (Wu et al., 2011) (Schmauss and Keppler, 2014). Interestingly, adsorption of SO₂ remains very strong at very low partial pressures, which confirms that adsorption is likely to happen in diluted cold parts of the plume (Schmauss and Keppler, 2014). Furthermore, an increase in sulfur load on ash surfaces was observed to increase with increase of distance from the vent during 2010 Eyjafjallajökull eruption (Bagnato et al., 2013). Thus, one can expect that most of the adsorption of SO₂ gas during a medium-size volcanic eruption would happen in the horizontal umbrella part of the volcanic ash cloud. In this case it is important to use the steady state uptake coefficient to evaluate the uptake as it is better fit to describe the phenomena of the continuous process. In this research it was demonstrated that even after 3 days of exposure of natural v-dust to the SO₂ gas there are still active sites available for the reaction to take place. Therefore one can expect a v-dust particle travelling through the air to remain active to the adsorption of SO₂ gas.

In order to evaluate potential impact of SO₂ adsorption on v-dust on atmosphere its atmospheric lifetime was calculated using equation (5).

$$\tau_{net} = \frac{4}{\gamma c D} \quad (5)$$

where γ is the uptake coefficient, c is the mean molecular velocity (m s⁻¹), and D is the volcanic dust surface area density (m² m⁻³). Considering (i) concentrations of volcanic ash in a vertical column of the volcanic cloud passing over Faroe Islands located about 650 km from the Eyjafjallajökull volcano measured during its eruption on April 15 2010 ranging from 200 to 6000 µg m⁻³ (Gudmundsson et al., 2012) and (ii) the SSA of Eyjafjallajökull dust sample of 0.75 m² g⁻¹, D can be calculated by direct multiplication of the dust concentration and the SSA of the v-dust and was found to be in the range from 1.5 × 10⁻⁴ m² m⁻³ to 4.5 × 10⁻³ m² m⁻³ for the lower and higher ash load respectively. This leads to the calculation of lifetime of SO₂ molecule as a result of its heterogeneous loss on Eyjafjallajökull v-dust particle to 81 to 2.7 years. If we consider a higher 7.5 m² g⁻¹ SSA values for Eyjafjallajökull dust obtained by Maters et al. the atmospheric lifetime falls to 8.1 years to 99 days (Maters et al., 2016). For comparison, the lifetime of SO₂ in the atmosphere as measured over the Eastern United States in the absence of volcanic activity ranges from 15 h in summer to 65 h in winter (Lee et al., 2011). On the base of these calculations it appears that the heterogeneous uptake of SO₂ molecule on the surface of v-dust particle is a negligible process in comparison with the gas phase oxidation by aqueous (i.e., H₂O₂) and gas-phase (i.e., OH) processes. However, in case of higher volcanic ash concentrations in the plume, for example 2.0 × 10⁶ µg m⁻³ estimated during 1991 Pinatubo eruption (SSA 1.5 m² g⁻¹ (Maters et al., 2016)) at the direct

proximity to the vent (Witham et al., 2012), and considering the same uptake coefficient measured in this study for Eyjafjallajökull, calculations lead to a radically shorter lifetime of 36 h and make heterogeneous uptake of SO₂ on volcanic dust particles equally important. Furthermore, the lifetime of SO₂ could be further decreased for volcanic particles with higher specific surface area. These calculations point out that adsorption of SO₂ on the surface of volcanic ash is most likely to happen in the part of volcanic cloud closest to the vent where ash concentration is the highest. The process of SO₂ loss due to heterogeneous reactions with v-dust particles could be further enhanced in the presence of oxidizing species (i.e., O₃, OH) and sunlight, and needs to be quantitatively evaluated.

Declaration of competing interest

The authors declare that they have no known competing financial interests or personal relationships that could have appeared to influence the work reported in this paper.

Acknowledgments

The authors acknowledge Mr Vincent Gaudion and Dr Mohamad Zeineddine (SAGE, IMT Lille Douai) for their assistance in the lab. We are grateful to Mr Bruno Malet and Dr Laurent Alleman (SAGE, IMT Lille Douai) for conducting the ICP-MS experiments. This work was achieved in the frame of Labex CaPPA, funded by ANR through the PIA under contract ANR-11-LABX-0005-01, and CPER CLIMIBIO project, both funded by the Hauts-de-France Regional Council and the European Regional Development Fund (ERDF). J. Lasne acknowledges support from the Labex CaPPA and CPER CLIMIBIO projects and the Hauts-de-France Regional Council for his post-doctoral fellowship.

Appendix A. Supplementary data

Supplementary data to this article can be found online at <https://doi.org/10.1016/j.atmosenv.2019.116942>.

References

- Harris, E., Sinha, B., Foley, S., Crowley, J.N., Borrmann, S., Hoppe, P., 2012. Sulfur isotope fractionation during heterogeneous oxidation of SO₂ on mineral dust. *Atmos. Chem. Phys.* 12, 4867–4884. <https://doi.org/10.5194/acp-12-4867-2012>.
- A Leed, E., Pantano, C., 2003. Computer modeling of water adsorption on silica and silicate glass fracture surfaces. *J. Non-Cryst. Solids* 325, 48–60. [https://doi.org/10.1016/S0022-3093\(03\)00361-2](https://doi.org/10.1016/S0022-3093(03)00361-2).
- Adams, J.W., Rodriguez, D., Cox, R.A., 2005. The uptake of SO₂ on Saharan dust: a flow tube study. *Atmos. Chem. Phys.* 5, 2679–2689. <https://doi.org/10.5194/acp-5-2679-2005>.
- Alleman, L.Y., Lamaison, L., Perdrix, E., Robache, A., Galloo, J.-C., 2010. PM10 metal concentrations and source identification using positive matrix factorization and wind sectoring in a French industrial zone. *Atmos. Res.* 96, 612–625. <https://doi.org/10.1016/j.atmosres.2010.02.008>.
- Andreae, M., 1995. *Climate Effects of Changing Atmospheric Aerosol*. World Survey of Climatology, vol. 16. Future Climates of the World, pp. 341–392 1995.
- Arnalds, O., Dagsson-Waldhauserova, P., Olafsson, H., 2016. The Icelandic volcanic aeolian environment: processes and impacts — a review. *Aeolian Res.* 20, 176–195. <https://doi.org/10.1016/j.aeolia.2016.01.004>.
- Ayris, P.M., Lee, A.F., Wilson, K., Kueppers, U., Dingwell, D.B., Delmelle, P., 2013. SO₂ sequestration in large volcanic eruptions: high-temperature scavenging by tephra. *Geochem. Cosmochim. Acta* 110, 58–69. <https://doi.org/10.1016/j.gca.2013.02.018>.
- Bagnato, E., Aiuppa, A., Bertagnini, A., Bonadonna, C., Cioni, R., Pistolesi, M., Pedone, M., Hoskuldsson, A., 2013. Scavenging of sulphur, halogens and trace metals by volcanic ash: the 2010 Eyjafjallajökull eruption. *Geochem. Cosmochim. Acta* 103, 138–160. <https://doi.org/10.1016/j.gca.2012.10.048>.
- Baltrusaitis, J., Cwiertny, D.M., Grassian, V.H., 2007. Adsorption of sulfur dioxide on hematite and goethite particle surfaces. *Phys. Chem. Chem. Phys.* 9, 5542–5554. <https://doi.org/10.1039/B709167B>.
- Baratoux, D., Mangold, N., Arnalds, O., Bardintzeff, J.-M., Platevoet, B., Grégoire, M., Pinet, P., 2011. Volcanic Sand in Iceland: diverse origins of aeolian sand deposits revealed at Dyngjúsandur and Lambahraun, Iceland. *Earth Surf. Process. Landforms* 36, 1789–1808. <https://doi.org/10.1002/esp.2201>.
- Brasseur, G.P., Granier, C., Walters, S., 1990. Future changes in stratospheric ozone and the role of heterogeneous chemistry. *Nature* 348, 626–628. <https://doi.org/10.1038/348626a0>.

- Clague, D.A., Denlinger, R.P., 1994. Role of olivine cumulates in destabilizing the flanks of Hawaiian volcanoes. *Bull. Volcanol.* 56, 425–434. <https://doi.org/10.1007/BF00302824>.
- Crowley, J.N., Ammann, M., Cox, R.A., Hynes, R.G., Jenkin, M.E., Melloouki, A., Rossi, M.J., Troe, J., Wallington, T.J., 2010. Evaluated kinetic and thermochemical data for atmospheric chemistry: volume V – heterogeneous reactions on solid substrates. *Atmos. Chem. Phys.* 10, 9059–9223. <https://doi.org/10.5194/acp-10-9059-2010>.
- Dagsson-Waldhauserova, P., Arnalds, O., Olafsson, H., 2014. Long-term variability of dust events in Iceland (1949–2011). *Atmos. Chem. Phys.* 14, 13411–13422. <https://doi.org/10.5194/acp-14-13411-2014>.
- Datta, A., Cavell, R.G., Tower, R.W., George, Z.M., 1985. Claus catalysis. 1. Adsorption of SO₂ on the alumina catalyst studied by FTIR and EPR spectroscopy. *J. Phys. Chem.* 89, 3. <https://doi.org/10.1021/j100249a014>.
- Deegan, F.M., 2010. *Processes of Magma-Crust Interaction Insights from Geochemistry and Experimental Petrology*. Acta Universitatis Upsaliensis, Uppsala.
- Delmelle, P., Wadsworth, F.B., Maters, E.C., Ayris, P.M., 2018. High temperature reactions between gases and ash particles in volcanic eruption plumes. *Rev. Mineral. Geochem.* 84, 285–308. <https://doi.org/10.2138/rmg.2018.84.8>.
- Diaz, L., Liauw, C.M., Edge, M., Allen, N.S., McMahon, A., Rhodes, N., 2005. Investigation of factors affecting the adsorption of functional molecules onto gel silicas. 1. Flow microcalorimetry and infrared spectroscopy. *J. Colloid Interface Sci.* 287, 379–387. <https://doi.org/10.1016/j.jcis.2004.09.039>.
- Dordevic, D., Tošić, I., Sakan, S., Petrović, S., Đuričić-Milanković, J., Finger, D., Waldhauserova, P., 2019. Can volcanic dust suspended from surface soil and deserts of Iceland be transferred to central Balkan similarly to African dust (Sahara)? *Front. Earth Sci.* 7, 142. <https://doi.org/10.3389/feart.2019.00142>.
- Durant, A.J., Shaw, R.A., Rose, W.I., Mi, Y., Ernst, G.G.J., 2008. Ice nucleation and over seeding of ice in volcanic clouds. *J. Geophys. Res.: Atmosphere* 113. <https://doi.org/10.1029/2007JD009064>.
- Durant, A.J., Bonadonna, C., Horwell, C.J., 2010. Atmospheric and environmental impacts of volcanic particulates. *Elements* 6, 235–240.
- Farges, F., Keppler, H., Flank, A.M., Lagarde, P., 2009. Sulfur K-edge XANES study of S sorbed onto volcanic ashes. *J. Phys. Conf. Ser.* 190, 012177. <https://doi.org/10.1088/1742-6596/190/1/012177>.
- Finlayson-Pitts Jr., B.J., J.N.P., 1999. *Chemistry of the Upper and Lower Atmosphere: Theory, Experiments, and Applications*. Elsevier.
- Gislason, S.R., Hassenkam, T., Nedel, S., Bovet, N., Eiríksdóttir, E.S., Alfredsson, H.A., Hem, C.P., Balogh, Z.I., Dideriksen, K., Óskarsson, N., Sigfusson, B., Larsen, G., Stipp, S.L.S., 2011. Characterization of Eyjafjallajökull volcanic ash particles and a protocol for rapid risk assessment. *Proc. Natl. Acad. Sci.* 108, 7307–7312. <https://doi.org/10.1073/pnas.1015053108>.
- Goodman, A.L., Li, P., Usher, C.R., Grassian, V.H., 2001. Heterogeneous uptake of sulfur dioxide on aluminum and magnesium oxide particles. *J. Phys. Chem. A* 105, 6109–6120. <https://doi.org/10.1021/jp004423z>.
- Groot Zwaartfink, C.D., Arnalds, Ó., Dagsson-Waldhauserova, P., Eckhardt, S., Prospero, J.M., Stohl, A., 2017. Temporal and spatial variability of Icelandic dust emissions and atmospheric transport. *Atmos. Chem. Phys.* 17, 10865–10878. <https://doi.org/10.5194/acp-17-10865-2017>.
- Gudmundsson, M.T., Thordarson, T., Höskuldsson, Á., Larsen, G., Björnsson, H., Prata, F.J., Oddsson, B., Magnússon, E., Högnadóttir, T., Petersen, G.N., Hayward, C.L., Stevenson, J.A., Jónsdóttir, I., 2012. Ash generation and distribution from the April–May 2010 eruption of Eyjafjallajökull, Iceland. *Sci. Rep.* 2, 572. <https://doi.org/10.1038/srep00572>.
- Hair, M.L., 1975. Hydroxyl groups on silica surface. *J. Non-Cryst. Solids Glass Surf.* 19, 299–309. [https://doi.org/10.1016/0022-3093\(75\)90095-2](https://doi.org/10.1016/0022-3093(75)90095-2).
- Highwood, E.-J., Stevenson, D.S., 2003. Atmospheric impact of the 1783–1784 Laki Eruption: Part II Climatic effect of sulphate aerosol. *Atmos. Chem. Phys.* 3, 1177–1189.
- Huang, L., Zhao, Y., Li, H., Chen, Z., 2015. Kinetics of heterogeneous reaction of sulfur dioxide on authentic mineral dust: effects of relative humidity and hydrogen peroxide. *Environ. Sci. Technol.* 49, 10797–10805. <https://doi.org/10.1021/acs.est.5b03930>.
- Hudson, P.K., Zondlo, M.A., Tolbert, M.A., 2002. The interaction of Methanol, acetone, and acetaldehyde with ice and nitric acid-doped ice: implications for cirrus clouds. *J. Phys. Chem. A* 106, 2882–2888. <https://doi.org/10.1021/jp012718m>.
- Huthwelker, T., Ammann, M., Peter, T., 2006. The uptake of acidic gases on ice. *Chem. Rev.* 106, 1375–1444. <https://doi.org/10.1021/cr02506v>.
- Ibrahim, S., Romanias, M.N., Alleman, L.Y., Zeineddine, M.N., Angeli, G.K., Trikalitis, P.N., Thevenet, F., 2018. Water interaction with mineral dust aerosol: particle size and hygroscopic properties of dust. *ACS Earth Space Chem.* 2, 376–386. <https://doi.org/10.1021/acsearthspacechem.7b00152>.
- Icelandic volcanoes [WWW Document], n.d. URL <http://icelandicvolcanoes.is/?volcano=EYJ#> (accessed 2.20.2019).
- Jiang, B.Q., Wu, Z.B., Liu, Y., Lee, S.C., Ho, W.K., 2010. DRIFT study of the SO₂ effect on low-temperature SCR reaction over Fe–Mn/TiO₂. *J. Phys. Chem. C* 114, 4961–4965. <https://doi.org/10.1021/jp907783g>.
- Joshi, N., Romanias, M.N., Riffault, V., Thevenet, F., 2017. Investigating water adsorption onto natural mineral dust particles: linking DRIFTS experiments and BET theory. *Aeolian Res.* 27, 35–45. <https://doi.org/10.1016/j.aeolia.2017.06.001>.
- Judeikis, H.S., Stewart, T.B., 1976. Laboratory measurement of SO₂ deposition velocities on selected building materials and soils. *Atmos. Environ.* 10, 769–776. 1967. [https://doi.org/10.1016/0004-6981\(76\)90078-0](https://doi.org/10.1016/0004-6981(76)90078-0).
- Kulkarni, D., Wachs, I.E., 2002. Isopropanol oxidation by pure metal oxide catalysts: number of active surface sites and turnover frequencies. *Appl. Catal. Gen.* 237, 121–137. [https://doi.org/10.1016/S0926-860X\(02\)00325-3](https://doi.org/10.1016/S0926-860X(02)00325-3).
- Langmann, B., 2013. Volcanic ash versus mineral dust: atmospheric processing and environmental and climate impacts. [WWW Document]. International Scholarly Research Notices. <https://doi.org/10.1155/2013/245076>.
- Langmann, B., Zakšek, K., Hort, M., 2010. Atmospheric distribution and removal of volcanic ash after the eruption of Kasatochi volcano: a regional model study. *J. Geophys. Res.: Atmosphere* 115. <https://doi.org/10.1029/2009JD013298>.
- Lasne, J., Romanias, M.N., Thevenet, F., 2018. Ozone uptake by clay dusts under environmental conditions. *ACS Earth Space Chem.* 2, 904–914. <https://doi.org/10.1021/acsearthspacechem.8b00057>.
- Lee, C., Martin, R.V., Donkelaar, A. van, Lee, H., Dickerson, R.R., Hains, J.C., Krotkov, N., Richter, A., Vinnikov, K., Schwab, J.J., 2011. SO₂ emissions and lifetimes: estimates from inverse modeling using in situ and global, space-based (SCIAMACHY and OMI) observations. *J. Geophys. Res.: Atmosphere* 116. <https://doi.org/10.1029/2010JD014758>.
- Li, L., Chen, Z.M., Zhang, Y.H., Zhu, T., Li, J.L., Ding, J., 2006. Kinetics and mechanism of heterogeneous oxidation of sulfur dioxide by ozone on surface of calcium carbonate. *Atmos. Chem. Phys. Discuss.* 6, 579–613. <https://doi.org/10.5194/acpd-6-579-2006>.
- Lo, J.M.H., Ziegler, T., Clark, P.D., 2010. SO₂ adsorption and transformations on γ -Al₂O₃ surfaces: a density functional theory study. *J. Phys. Chem. C* 114, 10444–10454. <https://doi.org/10.1021/jp910895g>.
- Massman, W.J., 1998. A review of the molecular diffusivities of H₂O, CO₂, CH₄, CO, O₃, SO₂, NH₃, N₂O, NO, and NO₂ in air O₂ and N₂ near STP. [WWW Document]. Atmospheric Environment. URL <https://eurekamag.com/research/008/072/008072627.php>, Accessed date: 11 May 2018.
- Maters, E.C., Delmelle, P., Rossi, M.J., Ayris, P.M., Bernard, A., 2016. Controls on the surface chemical reactivity of volcanic ash investigated with probe gases. *Earth Planet. Sci. Lett.* 450, 254–262. <https://doi.org/10.1016/j.epsl.2016.06.044>.
- Maters, E.C., Delmelle, P., Rossi, M.J., Ayris, P.M., 2017. Reactive uptake of sulfur dioxide and ozone on volcanic glass and ash at ambient temperature. *J. Geophys. Res. Atmos.* 122, 10077–10088. <https://doi.org/10.1002/2017JD026993>.
- Michigami, Y., Ueda, K., 1994. Sulphite stabilizer in ion chromatography. *J. Chromatogr. A* 663, 255–258. [https://doi.org/10.1016/0021-9673\(94\)85252-9](https://doi.org/10.1016/0021-9673(94)85252-9).
- Moroni, B., Arnalds, O., Dagsson-Waldhauserova, P., Crocchianti, S., Viviani, R., Cappelletti, D., 2018. Mineralogical and chemical records of Icelandic dust sources upon Ny-Ålesund (Svalbard islands). *Front. Earth Sci.* 6. <https://doi.org/10.3389/feart.2018.00187>.
- Nanayakkara, C.E., Pettibone, J., Grassian, V.H., 2012. Sulfur dioxide adsorption and photooxidation on isotopically-labeled titanium dioxide nanoparticle surfaces: roles of surface hydroxyl groups and adsorbed water in the formation and stability of adsorbed sulfate and sulfite. *Phys. Chem. Chem. Phys.* 14, 6957–6966. <https://doi.org/10.1039/C2CP23684B>.
- Ovadnevaite, J., Ceburnis, D., Plauskaite-Sukiene, K., Modini, R., Dupuy, R., Rimselyte, I., Ramonet, M., Kvietkus, K., Ristovski, Z., Berresheim, H., O'Dowd, C.D., 2009. Volcanic sulphate and arctic dust plumes over the North Atlantic Ocean. *Atmos. Environ.* 43, 4968–4974. <https://doi.org/10.1016/j.atmosenv.2009.07.007>.
- Reactions on Mineral Dust - Chemical Reviews [ACS Publications] [WWW Document], n.d. URL <https://pubs.acs.org/doi/abs/10.1021/cr020657y> (accessed 2.8.2018).
- Renggli, C., King, P., Henley, W.R., Guagliardo, P., McMorrow, L., Middleton, J., Turner, M., 2019. An experimental study of SO₂ reactions with silicate glasses and super-cooled melts in the system anorthite–diopside–albite at high temperature. *Contrib. Mineral. Petrol.* 174. <https://doi.org/10.1007/s00410-018-1538-2>.
- Romanias, M.N., El Zein, A., Bedjanian, Y., 2012. Heterogeneous interaction of H₂O₂ with TiO₂ surface under dark and UV light irradiation conditions. *J. Phys. Chem. A* 116, 8191–8200. <https://doi.org/10.1021/jp305366v>.
- Romanias, M.N., Ourrad, H., Thevenet, F., Riffault, V., 2016. Investigating the heterogeneous interaction of VOCs with natural atmospheric particles: adsorption of limonene and toluene on saharan mineral dusts. *J. Phys. Chem. A* 120, 1197–1212. <https://doi.org/10.1021/acs.jpca.5b10323>.
- Romanias, M.N., Zeineddine, M.N., Gaudion, V., Lun, X., Thevenet, F., Riffault, V., 2016. Heterogeneous interaction of isopropanol with natural Gobi dust. *Environ. Sci. Technol.* 50, 11714–11722. <https://doi.org/10.1021/acs.est.6b03708>.
- Schmaus, D., Keppler, H., 2014. Adsorption of sulfur dioxide on volcanic ashes. *Am. Mineral.* 99, 1085–1094. <https://doi.org/10.2138/am.2014.4656>.
- Schmidt, A., Witham, C.S., Theys, N., Richards, N.A.D., Thordarson, T., Szpek, K., Feng, W., Hort, M.C., Woolley, A.M., Jones, A.R., Redington, A.L., Johnson, B.T., Hayward, C.L., Carslaw, K.S., 2014. Assessing hazards to aviation from sulfur dioxide emitted by explosive Icelandic eruptions. *J. Geophys. Res. Atmos.* 119, 2014JD022070. <https://doi.org/10.1002/2014JD022070>.
- Shang, J., Li, J., Zhu, T., 2010. Heterogeneous reaction of SO₂ on TiO₂ particles. *Sci. China Chem.* 53, 2637–2643. <https://doi.org/10.1007/s11426-010-4160-3>.
- Stevenson, D.S., Johnson, C.E., Highwood, E.J., Gauci, V., Collins, W.J., Derwent, R.G., 2003. Atmospheric impact of the 1783–1784 Laki eruption: Part I Chemistry modelling. *Atmos. Chem. Phys.* 3, 487–507. <https://doi.org/10.5194/acp-3-487-2003>.
- Tambora and the “Year Without a Summer” of 1816, 2016. Institute of geography. WWW Document, URL http://www.geography.unibe.ch/services/geographica_bernenisia/online/gb2016g9001/index_eng.html, Accessed date: 17 May 2018.
- Tamura, H., Mita, K., Tanaka, A., Ito, M., 2001. Mechanism of hydroxylation of metal oxide surfaces. *J. Colloid Interface Sci.* 243, 202–207. <https://doi.org/10.1006/jcis.2001.7864>.
- Tang, M.J., Cox, R.A., Kalberer, M., 2014. Compilation and evaluation of gas phase diffusion coefficients of reactive trace gases in the atmosphere: volume 1. Inorganic compounds. *Atmos. Chem. Phys.* 14, 9233–9247. <https://doi.org/10.5194/acp-14-9233-2014>.
- Textor, C., Graf, H.-F., Herzog, M., Oberhuber, J.M., n.d. Injection of gases into the stratosphere by explosive volcanic eruptions. *Journal of Geophysical Research: Atmospheres* 108. <https://doi.org/10.1029/2002JD002987>.
- Thordarson, T., Larsen, G., 2007. Volcanism in Iceland in historical time: volcano types,

- eruption styles and eruptive history. *J. Geodyn.* 43, 118–152. <https://doi.org/10.1016/j.jog.2006.09.005>.
- Ullerstam, M., Vogt, R., Langer, S., Ljungstrom, E., 2002. The kinetics and mechanism of SO₂ oxidation by O₃ on mineral dust. *Phys. Chem. Chem. Phys.* 4, 4694–4699. <https://doi.org/10.1039/b203529b>.
- Usher, C.R., Al-Hosney, H., Carlos-Cuellar, S., Grassian, V.H., 2002. A laboratory study of the heterogeneous uptake and oxidation of sulfur dioxide on mineral dust particles. *J. Geophys. Res.* 107, 4713. <https://doi.org/10.1029/2002JD002051>.
- Vernier, J.-P., Fairlie, T.D., Deshler, T., Natarajan, M., Knepp, T., Foster, K., Wienhold, F. G., Bedka, K.M., Thomason, L., Trepte, C., n.d. In situ and space-based observations of the Kelud volcanic plume: The persistence of ash in the lower stratosphere. *J. Geophys. Res.: Atmosphere* 121, 11,104–11,118. <https://doi.org/10.1002/2016JD025344>.
- Vogel, A., Diplas, S., Durant, A.J., Azar, A.S., Sunding, M.F., Rose, W.I., Sytchkova, A., Bonadonna, C., Krüger, K., Stohl, A., 2017. Reference data set of volcanic ash physicochemical and optical properties. *J. Geophys. Res.: Atmosphere* 122, 9485–9514. <https://doi.org/10.1002/2016JD026328>.
- Wang, T., Liu, Y., Deng, Y., Fu, H., Zhang, L., Chen, J., 2018a. Emerging investigator series: heterogeneous reactions of sulfur dioxide on mineral dust nanoparticles: from single component to mixed components. *Environ. Sci.: Nano* 5, 1821–1833. <https://doi.org/10.1039/C8EN00376A>.
- Wang, T., Liu, Y., Deng, Y., Fu, H., Zhang, L., Chen, J.-M., 2018b. Adsorption of SO₂ on mineral dust particles influenced by atmospheric moisture. *Atmos. Environ.* 191. <https://doi.org/10.1016/j.atmosenv.2018.08.008>.
- Witham, C.S., Oppenheimer, C., Horwell, C.J., 2005. Volcanic ash-leachates: a review and recommendations for sampling methods. *J. Volcanol. Geotherm. Res.* 141, 299–326. <https://doi.org/10.1016/j.jvolgeores.2004.11.010>.
- Witham, C., Webster, H., Hort, M., Jones, A., Thomson, D., 2012. Modelling concentrations of volcanic ash encountered by aircraft in past eruptions. *Atmospheric Environment, Volcanic ash over Europe during the eruption of Eyjafjallajökull on Iceland. April-May 2010* 48, 219–229. <https://doi.org/10.1016/j.atmosenv.2011.06.073>.
- Wu, L.Y., Tong, S.R., Wang, W.G., Ge, M.F., 2011. Effects of temperature on the heterogeneous oxidation of sulfur dioxide by ozone on calcium carbonate. *Atmos. Chem. Phys.* 11, 6593–6605. <https://doi.org/10.5194/acp-11-6593-2011>.
- Zhang, Z., Ewing, G.E., 2002. Infrared spectroscopy of SO₂ aqueous solutions. *Spectrochim. Acta A Mol. Biomol. Spectrosc.* 58, 2105–2113.
- Zhang, X., Zhuang, G., Chen, J., Wang, Y., Wang, X., An, Z., Zhang, P., 2006. Heterogeneous reactions of sulfur dioxide on typical mineral particles. *J. Phys. Chem. B* 110, 12588–12596. <https://doi.org/10.1021/jp0617773>.
- Zhang, Y., Tong, S., Ge, M., Jing, B., Hou, S., Tan, F., Chen, Y., Guo, Y., Wu, L., 2018. The influence of relative humidity on the heterogeneous oxidation of sulfur dioxide by ozone on calcium carbonate particles. *Sci. Total Environ.* 633, 1253–1262. <https://doi.org/10.1016/j.scitotenv.2018.03.288>.
- Zhou, L., Wang, W., Gai, Y., Ge, M., 2014. Knudsen cell and smog chamber study of the heterogeneous uptake of sulfur dioxide on Chinese mineral dust. *J. Environ. Sci.* 26, 2423–2433. <https://doi.org/10.1016/j.jes.2014.04.005>.
- Zuo, Y., Chen, H., 2003. Simultaneous determination of sulfite, sulfate, and hydroxymethanesulfonate in atmospheric waters by ion-pair HPLC technique. *Talanta* 59, 875–881. [https://doi.org/10.1016/S0039-9140\(02\)00647-1](https://doi.org/10.1016/S0039-9140(02)00647-1).